Mechanical behaviour analysis of FGM plates on elastic foundation using a new exponential-trigonometric HSDT.

Fatima Z. Zaoui*[1], Djamel Ouinas[1], Abdelouahed Tounsi [2,3,4], Belkacem Achour[5], Jaime A. Viña Olay[6] and Tayyab A. Butt[5]

[1] *Laboratory of Science and Technology Environment and Valorization, Faculty of Sciences and Technology/Ibn Badis University, 27000 Mostaganem, Algeria.*
[2] *Material and Hydrology Laboratory, Civil Engineering Department, Faculty of Technology / Djilali Liabes University, 22000 Sidi Bel Abbes, Algeria.*
[3] *Department of Civil and Environmental Engineering, King Fahd University of Petroleum & Minerals, 31261 Dhahran, Eastern Province, Saudi Arabia.*
[4] *YFL (Yonsei Frontier Lab), Yonsei University, Seoul 03722, Korea*
[5] *Civil Engineering Department, University of Ha'il, KSA, Saudi Arabia.*
[6] *Department of Materials Science and Metallurgical Engineering, University of Oviedo, Viesques Campus,33203 Gijón, Asturias, Spain.*

(Received keep as blank, Revised keep as blank, Accepted keep as blank)

Abstract. In this research, a new two-dimensional (2D) and quasi three-dimensional (quasi-3D) higher order shear deformation theory is devised to address the bending problem of functionally graded plates resting on an elastic foundation. The displacement field of the suggested theories takes into account a parabolic transverse shear deformation shape function and satisfies shear stress free boundary conditions on the plate surfaces. It is expressed as a combination of trigonometric and exponential shear shape functions. The Pasternak mathematical model is considered for the elastic foundation. The material properties vary constantly across the FG plate thickness using different distributions as power-law, exponential and Mori–Tanaka model. By using the virtual works principle and Navier's technique, the governing equations of FG plates exposed to sinusoidal and evenly distributed loads are developed. The effects of material composition, geometrical parameters, stretching effect and foundation parameters on deflection, axial displacements and stresses are discussed in detail in this work. The obtained results are compared with those reported in earlier works to show the precision and simplicity of the current formulations. A very good agreement is found between the predicted results and the available solutions of other higher order theories. Future mechanical analyses of three-dimensionally FG plate structures can use the study's findings as benchmarks.

Keywords: Bending; Stress; Functionally graded plate; Shear deformation theory; Stretching effect, Winkler-Pasternak parameters.

1. Introduction

Functionally graded materials (FGMs) are a brand-new class of inhomogeneous composite materials that are created by combining metals and ceramics. These materials have incredible effectiveness since the mechanical properties of FGMs vary constantly along the thickness direction (Barretta *et al*. 2016, Rachid *et al*. 2022). These two material characteristics vary continuously and smoothly in the desired directions. FGM can thus not only combine the best qualities of ceramic and metal but also reduce residual and thermal stresses, both of which are quite frequent in traditional multi-layered composite systems (Mengzhen *et al*. 2021).

Owing to this characteristic, FGM have been investigated in numerous engineering applications including the aerospace, automotive, aviation and defence sectors, as well as more recently the electronic and biological applications (Nguyen 2015, Abdelhak 2016, Aldousari 2017). Due to the widespread use of FGM in engineering domains recently, a number of theories have been established

[1]* Corresponding author, Phd, E-mail: fatima.zaoui@univ-mosta.dz, tima22000@hotmail.com

to analyze the bending, buckling, and dynamic behaviors of diverse FG structures (Hebbar *et al*. 2020, Arefi and Allam 2015, Abdulrazzaq *et al*. 2020, Zaoui *et al.* 2021, 2022a). In order to study the free vibration of FG rectangular plates resting on elastic foundations, Mantari *et al*. (2014) introduced a new HSDT. Xiang and Kang (2013) carried out the bending analysis of functionally graded plates using an nth-order shear deformation theory. Based on an improved third-order shear deformation theory, Le *et al*. (2020) developed finite element formulations for analysing the vibration characteristics of FGSW plates partially supported by Pasternak foundation. For studying the static response of functionally graded plates resting on a Winkler-Pasternak foundation under a transverse uniform load or a sinusoidal distributed force, Benyoucef *et al*. (2010) introduced a novel hyperbolic shear deformation theory of plates. Using fewer unknowns, Thai and Kim (2013) used quasi-3D sinusoidal shear deformation theory to investigate the bending behaviour of FGM plates. The impact of porosity was studied utilizing the four variable plate theory for P- FGM plates with sinusoidal shape function. Based on Reddy's third-order shear deformation theory, Hosseini-Hashemi *et al*. (2011) introduced a novel exact closed-form approach to solve free vibration analysis of FG rectangular thick plates. Carrera *et al*. (2011) investigated the effects of thickness stretching in functionally graded plates and shells. Neves *et al*. suggested using quasi-3D sinusoidal and hyperbolic shear deformation theory to investigate the static and free vibration responses of FG plates (2012a, 2012b). Thai *et al*. (2013) investigated the bending, buckling and free vibration of FG thick plates resting on elastic foundation using a simple refined higher-order shear deformation theory with two variables. Jha *et al*. (2013) examined the free vibration behaviour of FG elastic, rectangular and simply supported plates using higher order shear/shear-normal deformation theories. Ouinas and Achour (2013) used the finite element approach to examine the buckling behavior of a square plate made of composite laminated material with an elliptical notch. Mantari and Soares (2015) presented the static response of advanced composite plates and shells utilizing quasi-3D non-polynomial sinusoidal higher-order shear deformation theories. Zhang *et al*. (2014) established a 3D elasticity solution for the bending of thick FG plates utilizing a hybrid semi-analytical approach—the state-space based differential quadrature method. Al-Khateeb and Zenkour (2014) used a revised shear and normal deformations plate theory to examine the effects of temperature and moisture on the bending behaviour of FG plates resting on elastic foundations. Mantari and Soares (2013) used a novel trigonometric higher-order theory that considers the stretching effect to develop an analytical solution for the static analysis of functionally graded plates. Lee *et al*. (2015) provided an improved higher order shear and normal deformation theory for E, P, and S-FGM plates on Pasternak elastic foundation. Using a new hyperbolic shape function, Akavci and Tanrikulu (2015) provided 2D and quasi-3D shear deformation theories for bending and free vibration analysis of single-layer FG plates. For the bending and free vibration analysis of functionally graded plates resting on elastic foundation, Mantari and Granados (2016) developed an original first shear deformation theory. To examine the static behavior of functionally graded single and sandwich beams with both shear deformation and stretching thickness effects, Yarasca *et al*. (2016) developed a Hermite-Lagrangian finite element formulation. Meftah *et al*. (2017) have conducted a free vibration analysis of FG plates on elastic foundations using a non-polynomial four refined shear deformation theory. To investigate the free vibration of functionally graded plates, Zaoui *et al*. (2017a) and Guerroudj *et al*. (2017) introduced hybrid quasi-3D shear deformation theories. Amar *et al*. (2018) developed a new, straightforward shear deformation theory with three unknowns for the static analysis of FG plates on elastic foundations. The bending, free vibration, and buckling behaviour of FG plates were investigated by Vu *et al*. (2019) utilizing a mesh-free technique and the inverse sin shear deformation plate theory. Levy type porous FGM plates' free vibration and bending analysis were examined by Demirhan and Taskin (2019).

For the purpose of assessing the bending and free vibrations of FGMs plates with simply supported edges, a novel quasi-3D trigonometric HSDTs with a new displacement field with indeterminate integral variables had been devised (Sidhoum *et al*. 2018, Zaoui *et al*. 2020, 2021, 2022b). Mahmoudi *et al*. (2018) examined the effect of micromechanical models on the free vibration of rectangular FGM plate resting on elastic foundation. Younsi *et al*. (2018) developed a non-polynomial 2D and quasi-3D theory to investigate static and dynamic responses of FG plates. Belkhodja *et al*. (2019) investigated the flexion, free vibrations and buckling of FGMs plate with simply supported edges using a new exponential-trigonometric shear function. For FGM plates with the stretching effect present, Bekhodja *et al*. (2022) introduced a novel quasi-3D and 2D hybrid (polynomial-hyperbolic-exponential) HSDT

with five unknowns of simply supported square or rectangular plates to study bending, free vibration, and buckling.

The main purpose of the present work is to implement a new 2D and quasi-3D shear strain theories to study the bending behaviour of FG plates simply supported and resting on elastic foundations of the Winkler-Pasternak type. The most intriguing aspect of this theory is that, in contrast to other theories like Neves *et al*. (2012a, 2012b), It has a new displacement field with fewer unknowns. In the proposed field of displacements, transverse shear and thickness stretching effects are taken into account in quasi-3D theory but ignored in the 2D model. Furthermore, in order to satisfy shear stress free boundary conditions without incorporating a shear correction factor, these theories take into account a parabolic variation of transverse shear stresses across the thickness. The fundamental governing equations for FG plates subjected to sinusoidal and uniformly distributed loads are established using the virtual work principle. Navier's method is used to generate closed-form deflection solutions for simply supported plates and the obtained results are then compared to those found in the literature to show the suggested theories' precision and clarity. The bending response of FG plates has been investigated in relation to the impacts of power-law index, slenderness ratio, side-to-thickness ratio, normal strain, Winkler-Pasternak parameters, various rules of mixture and boundary supports.

2. Analytical formulation

2.1. Material properties

In this study, a functionally graded rectangular plate with uniform thickness (h), length (a), width (b), is considered as shown in Fig. 1. The FGM material properties are supposed to change constantly according the plate thickness using the following rules of mixture

2.1.1 The power-law (P-FGM) variation

The volume fraction of the P-FGM plate changes conti-nuously across the thickness of the plate according to the power law variation (Zaoui et al., 2017b) as given in Eq. (1)

$$P(z) = P_m + (P_c - P_m)\left(\frac{1}{2} + \frac{z}{h}\right)^k \tag{1}$$

2.1.2 The exponential (E-FGM) variation

The E-FGM plate volume fraction vary continuously along the thickness direction of the plate according to the exponential distribution (Meradjah et al., 2018) as shown below

$$P(z) = Ae^{p(z+h/2)}, \quad A = P_m, \quad p = \frac{1}{h}\ln\left(\frac{P_c}{P_m}\right) \tag{2}$$

2.1.3 The Mori Tanaka Homogenization Model

For Mori–Tanaka scheme (Mori and Tanaka, 1973; Akavci and Tanrikulu, 2015), the volume fraction of the FGM plate is given in the following equation

$$P(z) = P_m + (P_c - P_m)\frac{V_c}{1 + V_m\left(\frac{P_c}{P_m} - 1\right)\frac{1+\nu}{3-3\nu}}, \tag{3a}$$

with

$$V_c = \left(\frac{1}{2} + \frac{z}{h}\right)^k, \quad V_m + V_c = 1 \tag{3b}$$

where P represents the effective material property like Young's modulus (E). The properties of the upper and bottom faces of the plate are designated by the letters P_m and P_c, respectively. k is the power law index. Poisson's ratio (ν) is assumed constant for all gradation models because its impact on the response of FG plates is relatively minimal.

2.2.Kinematics

Based on higher order shear deformation theory and considering the stretching effect, a novel displacement field of plates is developed as expressed below

$$\begin{aligned} u(x,y,z) &= u_0(x,y) - z\frac{\partial w_b}{\partial x} - f(z)\frac{\partial^3 w_s}{\partial x \partial y^2} \\ v(x,y,z) &= v_0(x,y) - z\frac{\partial w_b}{\partial y} - f(z)\frac{\partial^3 w_s}{\partial x^2 \partial y} \\ w(x,y,z) &= w_b(x,y) + w_s(x,y) + g(z)\phi_z(x,y) \end{aligned} \tag{4}$$

where u_0, v_0, w_b, w_s and φ_z are the five unknown displacement functions of mid plate surface. The form function $f(z)$ depicts how the transverse shear strains vary along the thickness. Note that $g(z) = 0$ for 2D problem.

The shape function utilized herein, is presented by Zaoui *et al*. (2019, 2022b) as

$$f(z) = \frac{\pi h}{\pi^4 + h^4} e^{(hz/\pi)}\left(\pi^2 \sin\left(\frac{\pi z}{h}\right) + h^2 \cos\left(\frac{\pi z}{h}\right)\right) - \frac{\pi h^3}{\pi^4 + h^4} \tag{5a}$$

$$\text{and } g(z) = \frac{df}{dz} \tag{5b}$$

The general strain – displacement relations can be defined from Eqs. (4) by the application of the linear, small-strain elasticity theory as follows

$$\begin{Bmatrix} \varepsilon_x \\ \varepsilon_y \\ \gamma_{xy} \end{Bmatrix} = \begin{Bmatrix} \varepsilon_x^0 \\ \varepsilon_y^0 \\ \gamma_{xy}^0 \end{Bmatrix} + z\begin{Bmatrix} k_x^b \\ k_y^b \\ k_{xy}^b \end{Bmatrix} + f(z)\begin{Bmatrix} k_x^s \\ k_y^s \\ k_{xy}^s \end{Bmatrix}, \tag{6a}$$

$$\begin{Bmatrix} \gamma_{yz} \\ \gamma_{xz} \end{Bmatrix} = \begin{Bmatrix} \gamma_{yz}^0 \\ \gamma_{xz}^0 \end{Bmatrix} + g(z)\begin{Bmatrix} \gamma_{yz}^1 \\ \gamma_{xz}^1 \end{Bmatrix}, \varepsilon_z = g'(z)\,\varepsilon_z^0 \tag{6b}$$

where

$$\left\{\begin{matrix}\varepsilon_x^0\\ \varepsilon_y^0\\ \gamma_{xy}^0\end{matrix}\right\}=\left\{\begin{matrix}\dfrac{\partial u_0}{\partial x}\\ \dfrac{\partial v_0}{\partial x}\\ \dfrac{\partial u_0}{\partial y}+\dfrac{\partial v_0}{\partial x}\end{matrix}\right\},\quad \left\{\begin{matrix}k_x^b\\ k_y^b\\ k_{xy}^b\end{matrix}\right\}=\left\{\begin{matrix}-\dfrac{\partial^2 w_b}{\partial x^2}\\ -\dfrac{\partial^2 w_b}{\partial y^2}\\ -2\dfrac{\partial^2 w_b}{\partial x\partial y}\end{matrix}\right\}, \tag{7a}$$

$$\left\{\begin{matrix}k_x^s\\ k_y^s\\ k_{xy}^s\end{matrix}\right\}=\left\{\begin{matrix}-\dfrac{\partial {w_s}^4}{\partial x^2\partial y^2}\\ -\dfrac{\partial {w_s}^4}{\partial x^2\partial y^2}\\ -\dfrac{\partial {w_s}^4}{\partial x\partial y^3}-\dfrac{\partial {w_s}^4}{\partial x^3\partial y}\end{matrix}\right\}, \tag{7b}$$

$$\left\{\begin{matrix}\gamma_{yz}^0\\ \gamma_{xz}^0\end{matrix}\right\}=\left\{\begin{matrix}\dfrac{\partial w_s}{\partial y}\\ \dfrac{\partial w_s}{\partial x}\end{matrix}\right\},\qquad \left\{\begin{matrix}\gamma_{yz}^1\\ \gamma_{xz}^1\end{matrix}\right\}=\left\{\begin{matrix}-\dfrac{\partial {w_s}^3}{\partial x^2\partial y}+\dfrac{\partial \phi_z}{\partial y}\\ -\dfrac{\partial {w_s}^3}{\partial x\partial y^2}+\dfrac{\partial \phi_z}{\partial x}\end{matrix}\right\}, \tag{7c}$$

$$\varepsilon_z^0=\varphi_z \text{ and } g'(z)=\frac{dg(z)}{dz} \tag{7d}$$

It can be seen from Eq. (6) that the transverse shear strains (γ_{xz} , γ_{yz}) are equal to zero at the top $\left(z=h/2\right)$ and bottom $\left(z=-h/2\right)$ surfaces of the plate. A shear correction coefficient is, hence, not required.

According to the three-dimensional (3D) elasticity, the stress-strain relationships for FG plates can be expressed as

$$\left\{\begin{matrix}\sigma_x\\ \sigma_y\\ \sigma_z\\ \tau_{yz}\\ \tau_{xz}\\ \tau_{xy}\end{matrix}\right\}=\left[\begin{matrix}Q_{11} & Q_{12} & Q_{13} & 0 & 0 & 0\\ Q_{12} & Q_{22} & Q_{23} & 0 & 0 & 0\\ Q_{13} & Q_{23} & Q_{33} & 0 & 0 & 0\\ 0 & 0 & 0 & Q_{44} & 0 & 0\\ 0 & 0 & 0 & 0 & Q_{55} & 0\\ 0 & 0 & 0 & 0 & 0 & Q_{66}\end{matrix}\right]\left\{\begin{matrix}\varepsilon_x\\ \varepsilon_y\\ \varepsilon_z\\ \gamma_{yz}\\ \gamma_{xz}\\ \gamma_{xy}\end{matrix}\right\} \tag{8}$$

The Q_{ij} expressions in terms of engineering constants are depends on the normal strain ε_z .

- In the case of quasi-3D HSDT's, $\varepsilon_z \neq 0$ then Q_{ij} are

$$Q_{11}=Q_{22}=Q_{33}=\frac{(1-\nu)E(z)}{(1-2\nu)(1+\nu)} \tag{9a}$$

$$Q_{12} = Q_{13} = Q_{23} = \frac{\nu\, E(z)}{(1-2\nu)(1+\nu)} \tag{9b}$$

$$Q_{44} = Q_{55} = Q_{66} = \frac{E(z)}{2(1+\nu)} \tag{9c}$$

- If the 2D HSDT is used, $\varepsilon_z = 0$ then Q_{ij} are

$$Q_{11} = Q_{22} = \frac{E(z)}{(1-\nu^2)} \tag{10a}$$

$$Q_{12} = \frac{\nu\, E(z)}{(1-\nu^2)} \tag{10b}$$

$$Q_{44} = Q_{55} = Q_{66} = \frac{E(z)}{2(1+\nu)} \tag{10c}$$

For FG plates, the constitutive relations (8) can be used to precisely calculate the in-plane normal and shear stresses (σ_x , σ_y and τ_{xy}). However, the boundary conditions at the upper and lower plate surfaces may notbe respected if the transverse normal and shear stresses (σ_z , τ_{yz} and τ_{xz}) derived from these constitutive relations. Hence, these stresses are calculated by integrating the 3D elasticity equilibrium equations with respect to the thickness coordinate as

$$\tau_{xz} = -\int_{-h/2}^{z}\left(\frac{\partial\sigma_x}{\partial x} + \frac{\partial\tau_{xy}}{\partial y}\right)dz + C_1(x,y) \tag{11a}$$

$$\tau_{yz} = -\int_{-h/2}^{z}\left(\frac{\partial\tau_{xy}}{\partial x} + \frac{\partial\sigma_y}{\partial y}\right)dz + C_2(x,y) \tag{11b}$$

$$\begin{aligned}\sigma_z = &-\int_{-h/2}^{z}\left(\int_{-h/2}^{z}\left[\frac{\partial^2\sigma_x}{\partial x^2} + 2\frac{\partial^2\tau_{xy}}{\partial x\partial y} + \frac{\partial^2\sigma_y}{\partial y^2}\right]dz\right)dz \\ &+ C_3(x,y)\,z + C_4(x,y)\end{aligned} \tag{11c}$$

where C's (i=1, 4) are constants that are specified by the upper and lower boundary conditions of the plate, which are expressed as follows.

$$\tau_{xz}\big|_{z=\pm h/2} = 0,\ \tau_{yz}\big|_{z=\pm h/2} = 0,\ \sigma_z\big|_{z=h/2} = q(x,y), \sigma_z\big|_{z=-h/2} = 0 \tag{12}$$

2.3. *Equilibrium equations and stress components*

By using the concept of virtual works, it is possible to construct the equilibrium equations of functionally graded plate subjected to mechanical applied loads, which can be written analytically as

$$\int_{-h/2}^{h/2}\int_{A}\left(\sigma_x\,\delta\,\varepsilon_x+\sigma_y\,\delta\,\varepsilon_y+\sigma_z\,\delta\,\varepsilon_z+\tau_{xy}\,\delta\,\gamma_{xy}+\tau_{yz}\,\delta\,\gamma_{yz}+\tau_{xz}\,\delta\,\gamma_{xz}\right)dA\,dz$$
$$-\int_{A}\left(q-f_e\right)\delta\,w\,dA\,dz=0 \tag{13}$$

Where A is the top surface, q is the external load applied to the plate and f_e is the density of foundation reaction effort. For the Pasternak foundation model;

$$f_e=K_w w-K_{sx}\frac{\partial^2 w}{\partial x^2}-K_{sy}\frac{\partial^2 w}{\partial y^2} \tag{14}$$

where K_w is the transverse elastic coefficient of the foundation and K_{sx}, K_{sy} are coefficients of the shear layer foundation stiffness. If the foundation is homogeneous and isotropic, this means that $K_{sx}=K_{sy}=K_s$. The Winkler foundation replaces the Pasternak foundation if the stiffness of the shear layer foundation is ignored.

By replacing Eqs. (6) and (8) in Eq. (13) and integrating over the thickness of the plate, Eq. (13) can be expressed as

$$\int_{A}\Big[N_x\,\delta\varepsilon_x^0+N_y\,\delta\varepsilon_y^0+N_z\,\delta\varepsilon_z^0+N_{xy}\,\delta\gamma_{xy}^0+M_x^b\,\delta k_x^b+M_y^b\,\delta k_y^b+M_{xy}^b\,\delta k_{xy}^b$$
$$+M_x^s\,\delta k_x^s+M_y^s\,\delta k_y^s+M_{xy}^s\delta k_{xy}^s+M_{xz}\delta\gamma_{yz}^0+M_{yz}\delta\gamma_{xz}^0+Q_{yz}^s\delta\gamma_{xz}^1+Q_{xz}^s\delta\gamma_{yz}^1\Big]dA \tag{15}$$
$$-\int_{A}\left(q-f_e\right)\left(\delta w_b+\delta w_s\right)dA=0$$

The stress resultants N, M and Q are given by

$$\left(N_i,M_i^b,M_i^s\right)=\int_{-h/2}^{h/2}\left(1,z,f\right)\sigma_i\,dz,\ (i=x,y,xy) \tag{16a}$$

$$N_z=\int_{-h/2}^{h/2}g'(z)\,\sigma_z\,dz \tag{16b}$$

$$\left(Q_{xz}^s,Q_{yz}^s\right)=\int_{-h/2}^{h/2}g\left(\tau_{xz},\tau_{yz}\right)dz \tag{16c}$$

By substituting Eqs. (7) into Eq. (13), integrating the displacement terms in parts and putting the coefficients δu_0, δv_0, δw_b, δw_s and $\delta\varphi_z$ to zero, independently, the governing equations of equilibrium can be constructed as follows

$$\delta u_0\ :\ \frac{\partial N_x}{\partial x}+\frac{\partial N_{xy}}{\partial y}=0 \tag{17a}$$

$$\delta v_0\ :\ \frac{\partial N_y}{\partial y}+\frac{\partial N_{xy}}{\partial x}=0 \tag{17b}$$

$$\delta w_b : \frac{\partial^2 M_x^b}{\partial x^2} + \frac{\partial^2 M_y^b}{\partial y^2} + 2\frac{\partial^2 M_{xy}^b}{\partial x \partial y} - f_e + q = 0 \tag{17c}$$

$$\delta w_s : \frac{\partial^4 M_x^s}{\partial x^2 \partial y^2} + \frac{\partial^4 M_y^s}{\partial x^2 \partial y^2} + \frac{\partial^4 M_{xy}^s}{\partial x \partial y^3} + \frac{\partial^4 M_{xy}^s}{\partial x^3 \partial y} + \frac{\partial M_{xz}}{\partial x} + \frac{\partial M_{yz}}{\partial y} - \frac{\partial^3 Q_{xz}^s}{\partial x^2 \partial y} - \frac{\partial Q_{yz}^s}{\partial x \partial y^2} = 0 \tag{17d}$$

$$\delta \varphi_z : \frac{\partial S_{xz}^s}{\partial x} + \frac{\partial S_{yz}^s}{\partial y} - N_z = 0 \tag{17e}$$

The stresses and moment resultants given in Eqs. (15) can be formulated in terms of generalized displacements (δu_0, δv_0, δw_b, δw_s and $\delta \varphi_z$) by substituting Eq. (5) into Eq. (16) and integrating through the thickness of the plate, as

$$\begin{Bmatrix} N_x \\ N_y \\ N_{xy} \\ M_x^b \\ M_y^b \\ M_{xy}^b \\ M_x^s \\ M_y^s \\ M_{xy}^s \\ N_z \end{Bmatrix} = \begin{bmatrix} A_{11} & A_{12} & 0 & B_{11} & B_{12} & 0 & B_{11}^s & B_{12}^s & 0 & X_{13} \\ A_{12} & A_{22} & 0 & B_{12} & B_{22} & 0 & B_{12}^s & B_{22}^s & 0 & X_{23} \\ 0 & 0 & A_{66} & 0 & 0 & B_{66} & 0 & 0 & B_{66}^s & 0 \\ B_{11} & B_{12} & 0 & D_{11} & D_{12} & 0 & D_{11}^s & D_{12}^s & 0 & Y_{13} \\ B_{12} & B_{22} & 0 & D_{12} & D_{22} & 0 & D_{12}^s & D_{22}^s & 0 & Y_{23} \\ 0 & 0 & B_{66} & 0 & 0 & D_{11} & 0 & 0 & D_{66}^s & 0 \\ B_{11}^s & B_{12}^s & 0 & D_{11}^s & D_{12}^s & 0 & H_{11}^s & H_{12}^s & 0 & Y_{13}^s \\ B_{12}^s & B_{22}^s & 0 & D_{12}^s & D_{22}^s & 0 & H_{12}^s & H_{22}^s & 0 & Y_{23}^s \\ 0 & 0 & B_{66}^s & 0 & 0 & D_{66}^s & 0 & 0 & H_{66}^s & 0 \\ X_{13} & X_{23} & 0 & Y_{13} & Y_{23} & 0 & Y_{13}^s & Y_{23}^s & 0 & Z_{33} \end{bmatrix} \begin{Bmatrix} \varepsilon_x^0 \\ \varepsilon_y^0 \\ \gamma_{xy}^0 \\ k_x^b \\ k_y^b \\ k_{xy}^b \\ k_x^s \\ k_y^s \\ k_{xy}^s \\ \varepsilon_z^0 \end{Bmatrix} \tag{18a}$$

$$\begin{Bmatrix} M_{yz} \\ M_{xz} \\ Q_{yz}^s \\ Q_{xz}^s \end{Bmatrix} = \begin{bmatrix} A_{44} & 0 & A_{44}^s & 0 \\ 0 & A_{55} & 0 & A_{55}^s \\ A_{44}^s & 0 & A_{44}^{st} & 0 \\ 0 & A_{55}^s & 0 & A_{55}^{st} \end{bmatrix} \begin{Bmatrix} \gamma_{yz}^0 \\ \gamma_{xz}^0 \\ \gamma_{yz}^1 \\ \gamma_{xz}^1 \end{Bmatrix} \tag{18b}$$

where the stiffness components and inertias are given as

$$\left(A_{ij}, A_{ij}^s, B_{ij}, D_{ij}, B_{ij}^s, D_{ij}^s, H_{ij}^s\right) = \int_{-h/2}^{h/2} Q_{ij}\left(1, g^2(z), z, z^2, f(z), z\ f(z), f^2(z)\right) dz \tag{19a}$$

$$\left(X_{ij}, Y_{ij}, Y_{ij}^s, Z_{ij}\right) = \int_{-h/2}^{h/2} \left(1, z, f(z), g'(z)\right) g'(z)\, Q_{ij}\, dz \tag{19b}$$

3. Navier-type solutions for simply supported FG plates

The Navier's procedure (Shao and Ma, 2007; Grover et al., 2013), based on double Fourier series, is employed herein to define the closed-form solution of the partial differential equations (Eqs.(18)) for which the displacement variables satisfying the boundary conditions can be given as

$$\begin{Bmatrix} u_0 \\ v_0 \\ w_b \\ w_s \\ \phi_z \end{Bmatrix} = \sum_{m=1}^{\infty}\sum_{n=1}^{\infty} \begin{Bmatrix} U_{mn}\cos(\lambda x)\sin(\mu y) \\ V_{mn}\sin(\lambda x)\cos(\mu y) \\ W_{bmn}\sin(\lambda x)\sin(\mu y) \\ W_{smn}\sin(\lambda x)\sin(\mu y) \\ \Phi_{mn}\sin(\lambda x)\sin(\mu y) \end{Bmatrix} \tag{20}$$

where $(U_{mn}, V_{mn}, W_{bmn}, W_{smn}, \Phi_{mn})$ are unknown functions to be determined. λ and μ are expressed as

$$\lambda = m\pi / a \text{ and } \mu = n\pi / b \tag{21}$$

The transverse distributed load $q(x, y)$ is also expanded in a double-Fourier series as

$$q(x,y) = \sum_{m=1}^{\infty}\sum_{n=1}^{\infty} q_{mn}\sin\left(\frac{m\pi}{a}x\right)\sin\left(\frac{n\pi}{b}y\right) \tag{22}$$

The coefficients q_{mn} are given below for some general loadings

- For uniformly distributed load

$$q_{mn} = \begin{cases} \dfrac{16q_0}{mn\pi^2}, & m, n = 1,3,5,..... \\ 0 & m, n = 2,4,6,..... \end{cases} \tag{23}$$

- For sinusoidal distributed load

$$q_{mn} = q_0 \tag{24}$$

in which q_0 is the intensity of the load.

In order to obtain closed-form solutions (Eq. (25)) for the static issue of the FG plate, Eqs. (18), (20) and (22) must be substituted into Eq. (17).

$$\begin{bmatrix} S_{11} & S_{12} & S_{13} & S_{14} & S_{15} \\ S_{12} & S_{22} & S_{23} & S_{24} & S_{25} \\ S_{13} & S_{23} & S_{33} & S_{34} & S_{35} \\ S_{14} & S_{24} & S_{34} & S_{44} & S_{45} \\ S_{15} & S_{25} & S_{35} & S_{45} & S_{55} \end{bmatrix} \begin{Bmatrix} U_{mn} \\ V_{mn} \\ W_{bmn} \\ W_{smn} \\ \Phi_{mn} \end{Bmatrix} = \begin{Bmatrix} 0 \\ 0 \\ q_{mn} \\ q_{mn} \\ 0 \end{Bmatrix} \tag{25}$$

in which

$$\begin{aligned} &S_{11} = \lambda^2 A_{11} + \mu^2 A_{66},\ S_{12} = \lambda\mu\left(A_{12} + A_{66}\right) \\ &S_{13} = -\lambda^3 B_{11} - \lambda\mu^2\left(B_{12} + 2B_{66}\right) \\ &S_{14} = \lambda^3\mu^2\left(B_{11}^s + B_{12}^s\right) + \left(\lambda\mu^4 + \lambda^3\mu^2\right)B_{66}^s \\ &S_{15} = -\lambda X_{13} \end{aligned} \tag{26}$$

$$S_{22} = \lambda^2 A_{66} + \mu^2 A_{22}$$
$$S_{23} = -\mu^3 B_{22} - \lambda^2 \mu \left(B_{12} + 2B_{66} \right)$$
$$S_{24} = \lambda^2 \mu^3 \left(B_{12}^s + B_{22}^s \right) + \left(\lambda^2 \mu^3 + \lambda^4 \mu \right) B_{66}^s$$
$$S_{25} = -\mu X_{23}$$
$$S_{33} = \lambda^4 D_{11} + \mu^4 D_{22} + 2\lambda^2 \mu^2 (D_{12} + 2D_{66}) + K_w + \lambda^2 K_{sx} + \mu^2 K_{sy}$$
$$S_{34} = -\lambda^2 \mu^2 \left(\lambda^2 D_{11}^s + \mu^2 D_{22}^s \right) + \left(\lambda^2 \mu^4 + \lambda^4 \mu^2 \right) \left(D_{12}^s + 2D_{66}^s \right) - 2\alpha^2 \beta^2 \left(k_1 A' + k_2 B' \right) D_{66}^s$$
$$S_{35} = \lambda^2 Y_{13} + \mu^2 Y_{23}$$
$$S_{44} = \lambda^4 \mu^4 \left(H_{11}^s + 2H_{12}^s + H_{22}^s + 2H_{66}^s \right) + \lambda^2 \mu^2 \left(\lambda^4 + \mu^4 \right) H_{66}^s + 2\lambda^2 \mu^2 \left(As_{44} + As_{55} \right) + \lambda^2 \mu^2 \left(\mu^2 Ast_{55} + \lambda^2 Ast_{44} \right)$$
$$S_{45} = \lambda^2 \mu^2 \left(Ast_{55}^s + Ast_{44}^s - Y_{13}^s - Y_{23}^s \right) + \lambda^2 A_{55}^s + \mu^2 A_{44}^s$$
$$S_{55} = \lambda^2 A_{55}^s + \mu^2 A_{44}^s + Z_{33}$$

4.Results and Discussion

4.1. Bending study of FG plates with simple supports

The accuracy of the current theory in analyzing thebending behavior of simply supported FG plates is examined in this section through the presentation of several numerical examples and comparison with the findings of various 2D, 3D, and quasi-3D shear deformation theories. Table 1 lists the mechanical properties of the metal and ceramic materials employed in this study. Both homogeneous isotropic plates and FGPs are investigated in the computations, and parameters study were also establshed. The numerical findings are presented in graphical and tabular forms by using the following non-dimensional displacements and stresses

$$\bar{w} = \frac{10h^3 E_c}{a^4 q_0} w\left(\frac{a}{2}, \frac{b}{2}, z\right),\ \bar{\sigma}_x = \frac{h}{aq_0}\sigma_x\left(\frac{a}{2}, \frac{b}{2}, z\right),\ \bar{\sigma}_y = \frac{h}{aq_0}\sigma_y\left(\frac{a}{2}, \frac{b}{2}, z\right),$$
$$\bar{\tau}_{xy} = \frac{h}{aq_0}\tau_{xy}(0,0,z),\ \bar{\tau}_{xz} = \frac{h}{aq_0}\tau_{xz}\left(0, \frac{b}{2}, z\right),\ \bar{\tau}_{yz} = \frac{h}{aq_0}\tau_{yz}\left(\frac{a}{2}, 0, z\right)$$
$$\tilde{u} = \frac{E_c}{hq_0} u\left(0, \frac{b}{2}, z\right),\ \tilde{w} = \frac{E_c}{hq_0} w\left(\frac{a}{2}, \frac{b}{2}, z\right),\ \tilde{\sigma}_x = \frac{\sigma_x\left(\frac{a}{2}, \frac{b}{2}, z\right)}{q_0},$$
$$\tilde{\sigma}_z = \frac{\sigma_z\left(\frac{a}{2}, \frac{b}{2}, z\right)}{q_0}, \tilde{\tau}_{xy} = \frac{\tau_{xy}(0,0,z)}{q_0},\ \tilde{\tau}_{xz} = \frac{\tau_{xz}\left(0, \frac{b}{2}, z\right)}{q_0} \tag{27}$$
$$\hat{u} = \frac{G_1}{hq_0} u\left(0, \frac{b}{2}, z\right),\ \hat{w} = \frac{G_1}{hq_0} w\left(\frac{a}{2}, \frac{b}{2}, z\right),$$

4.1.1. *Functionally graded plates (P-FGM)*

In this section, non-dimensional displacements and stresses of an Al/Al_2O_3 FG square plate under uniformly and sinusoidal distributed loads for various values of the power-law index are calculated and presented in Tables 2 and 3.

In Table 2, the computed results of non-dimensional deflection and stress components of moderately thick square FG plate under uniform load are compared with those given by quasi-3D and 2D shear deformation theories by Akavci and Tanrikulu (2015) and Younsi et al. (2018). From this table, it can be observed that the results of the proposed 2D theory agree well with those of Akavci and Tanrikulu (2015) and Younsi et al. (2018) in all cases. Besides, by comparing the obtained values by the present quasi-3D theory with those given by the other quasi-3D theories, an excellent correlation can be remarked.

Table 3presents the non-dimensional normal stress $(\bar{\sigma}_x)$ and transverse displacement $(\bar{w})$ of square thin and thick plates subjected to sinusoidal load forthree different power law index (k). The predicted results are compared with those generated by Carerra et al. (2011) based on a fourth-order variations of both in-plane and transverse displacements across the thickness, quasi-3D sinusoidal and hyperbolic shear deformation theories of Neves et al. (2012a, 2012b), quasi-3D shear deformation theories of Hebali (2014), 2D and quasi-3D hyperbolic shear deformation theories of Akavci and Tanrikulu (2015) and Younsi et al. (2018). A good agreement between the results is found for both thin and thick plates. Also, the present model provides a good prediction of both displacement and stress even in thick FG plates where the stretching effects are more pronounced.

Moreover, it should be noticed that the number of unknown variables used in the present formulation is just four in the 2D theory and five in the quasi-3D model, while nine unknown functions were used in hyperbolic shear deformation theories of Neves et al. (2012a, 2012b). It can be concluded that the present theory is not only accurate but also comparatively simple in predicting the bending response of simply supported FGM plates.

The stresses and displacements variations through the thickness of Al/Al_2O_3 FG square plate subjected to sinusoidal load are plotted in Fig. 2. The results are shown as compared with the quasi-3D shear deformation theory of Akavci and Tanrikulu (2015) for different values of power-law index (k). From this figure, it can be observedan excellent agreement between the obtained results and those computed by Akavci and Tanrikulu (2015). It is important to stress out that, the in-plane stresses $(\bar{\sigma}_x)$ and $(\bar{\tau}_{xy})$ exhibit linear variation through the thickness of homogeneous plate while it is parabolic for FG plates. This figure also shows that, the deflection $(\bar{w})$ and in-plane stresses $(\bar{\sigma}_x)$ and $(\bar{\sigma}_y)$ increase and the shear stresses $(\bar{\tau}_{xz})$ and $(\bar{\tau}_{xy})$ diminish with the increasing value of material index (k) .

Fig. 3 presents a 3D interaction diagram of the power-law index (k), side-to-thickness ratio (a/h) and center deflection $(\bar{w})$ using the proposed 2D and quasi-3D theories. It can be seen from this figure that the center deflection increases with the increase of the power-law index and decreases with the increasing of the thickness ratio. It is due to the fact that a higher value of (k) corresponds to lower value of volume fraction of the ceramic phase, and thus leads to the decrease of the value of the elasticity modulus which makes the plate softer. It also can be shown that the center deflections computed from the present 2D theory which neglect the thickness stretching effect are higher than those calculated from quasi-3D theory.

4.1.2. *Exponentially graded plates (E-FGM)*

Computations in this section are carried out for a simply supported E-FGM plate. The material properties of the E-FGM plate are defined by the exponential function given in Eq. (2). The non-dimensional stress and displacements of the E-FGM plate are calculated and compared with the results of different HSDTs for different loadings.

The center deflections $(\bar{w})$, in-plane and transverse shear stresses $(\bar{\sigma}_x, \bar{\tau}_{xz})$ of Al/Al_2O_3 plates under sinusoidal loads are calculated for different values of aspect ratio (b/a), thickness ratio (a/h) and exponent values (k) in Tables 4-6. The central deflections of the very thick E-FGM plates are

analyzed in Table 4. The obtained predictions are compared with the quasi-3D sinusoidal and exact 3D elasticity theories of Zenkour (2007), 2D and quasi-3D trigonometric models of Mantari and Soares (2013) and the quasi-3D and 2D shear deformation theories by Akavci and Tanrikulu (2015), Younsi et al. (2018). Since the proposed and other quasi-3D models include the thickness-stretching influence, they lead to results close to each other. Whereas, 2D HSDTs overestimate the deflections due to omitting the thickness stretching influence. In Tables 5 and 6, the computed non-dimensional stresses are provided as compared with those given by Younsi et al. (2018), Akavci and Tanrikulu (2015) based on quasi-3D and 2D hyperbolic theories and Mantari and Soares (2013) using 2D and quasi-3D trigonometric theories. It can be seen from the table that an excellent agreementis achieved between the results of present theory and those of other theories. Tables 4–6 demonstrate also that deflection $(\overline{w})$ and transverse shear stress $(\bar{\tau}_{xz})$ diminish and in plane stress $(\bar{\sigma}_x)$ increases with the increase of the exponent (k).

In Fig. 4, the variation of non-dimensional displacements and stresses according to the thickness of an E-FGM plate subjected to sinusoidal loading for different E_0/E_1 ratios are displayed using the present theory with including the thickness stretching effect and compared with the quasi-3D theory of Younsi et al. (2018). A very good accuracy between the solutions is observed. It can be seen also from these results that the non-dimensional displacements increase with the increasing of E_0/E_1. In addition, it can be deduced that E_0/E_1 ratios affect considerably the non-dimensional stresses.

4.1.3. *Comparative study*

In this party, parametric studies have been presented to evaluate the effect of power law index (k) and side-to-thickness ratio (a/h) on the bending of functionally graded plates using three rules of mixture (P-FGM, E-FGM, Mori-Tanaka homogenization model). Fig. 5 illustrates the variation of non-dimensional deflection $(\overline{w})$with respect to exponent index (k) and slenderness ratio (a/h) for P-FGM, E-FGM, Mori-Tanaka homogenization scheme. It can be noted from this figure, that deflections of plates using E-FGM decrease and by using P-FGM and Mori-Tanaka homogenization model increase when the exponent index increases. Such behavior is due to the fact that the increase of power-law index will increase the stiffness of the EGM plate, and thus, lead to a reduction of transverse displacement.

Fig. 6 is devoted to present the influence of side-to-thickness ratio on non-dimensional deflection of simply supported plate with different models. As can be observed from this figure, increasing of side-to-thickness ratio causes reducing of the magnitude of deflection, it means that the effect of shear deformation is significant when plates are thick $(a/h \le 5)$ and negligible for thin plates. Further, it is apparent that plates made with exponential function have the lowest deflection than the other functions.

Another comparative study for evaluating the dimensionless center deflections of Mori-Tanaka homogenization scheme, P-FGM and E-FGM plates subjected to sinusoidal load is carried out. From Fig. 7, it is showed that the deflection at the center of plates with Mori-Tanaka homogenization model is larger than those of P-FGM and E-FGM plates. The E-FGM plate which has the smallest deflection is stiffer than the other FGM plates.

4.2. *Analysis of FG plates on elastic foundation*

This section aims to demonstrate the accuracy of the proposed new models in predicting the static response of FG plates resting on elastic foundation.The following relations of non-dimensional displacements, stresses and foundation parameters in the bending problem are used

$$u^* = \frac{100D_c}{q_0 a^4} u\left(0, \frac{b}{2}, -\frac{h}{2}\right),\ v^* = \frac{100D_c}{q_0 a^4} v\left(\frac{b}{2}, 0, -\frac{h}{2}\right),$$

$$w^* = \frac{100D_c}{q_0 a^4} w\left(\frac{a}{2}, \frac{b}{2}\right),\ \sigma_x* = -\frac{h^2}{q_0 a^2}\sigma_x\left(\frac{a}{2}, \frac{b}{2}, -\frac{h}{2}\right)$$

$$\sigma_y * = -\frac{h^2}{q_0 a^2}\sigma_y\left(\frac{a}{2},\frac{b}{2},-\frac{h}{2}\right),\ \sigma_{xy} * = \frac{h^2}{q_0 a^2}\sigma_{xy}\left(0,0,-\frac{h}{2}\right) \tag{28}$$

$$K_0 = \frac{K_w a^4}{E_0 h^3},\ J_0 = \frac{K_s a^2}{\nu E_0 h^3},\ E_0 = 1GPa$$

$$\overline{K}_w = \frac{K_w a^4}{D_c},\ \overline{K}_s = \frac{K_s a^2}{D_c},\ D_c = \frac{E_c h^3}{12(1-\upsilon^2)}$$

In the first example, isotropic square plates on elastic foundation are analyzed to verify the accuracy of the proposed theories. The dimensionless deflection of homogeneous square plate subjected to uniform loads is presented in Table 8 for two values of the side-to-thickness ratio (a/h) and different values of the foundation parameters $(\overline{K}_w, \overline{K}_s)$. The obtained results are compared with those given by Thai and Choi (2014a) using differential quadrature method and those of Al Khateeb and Zenkour (2014) based on refined shear deformation plate theory. This table proves that the computed results are in excellent agreement with those reported by the other theories of Thai and Choi (2014a), Al Khateeb and Zenkour (2014) for all values of side-to-thickness ratio and foundation parameters.

The next example is implemented for Al/Al_2O_3 moderately thick rectangular plates on elastic foundation. Table 9 presents a comparison of non-dimensional displacements and stresses of FG plate for various exponent value (k) and foundation parameters (K_0, J_0) derived from the present theory, the sinusoidal shear deformation theory of Zenkour (2009), the 2D Zeroth-order shear deformation theory of Thai and Choi (2014a) and the first shear deformation theory of Mantari and Granados (2016). It is explicit that the present results are again found more close in all cases. It should be noted thatthe present theory is not only efficient but more accurate in predicting the bending behavior of FG plates resting on elastic foundation. The table exhibits that, axial displacements, deflection and stresses decreases with the increase of foundation parameters. In addition, it is apparent that the computed values from the present quasi-3D theory which takes into account the thickness stretching effect are smaller than those calculated from 2D theory.

To check the effect of Winkler's and Pasternak's foundation parameters $(\overline{K}_w, \overline{K}_x)$ on the bending behavior of FG plates subjected to sinusoidal loads based on the proposed 2D and quasi-3D theories, Fig. 8 depicts the variation of non-dimensional deflection $(\overline{w})$ of Al/Al_2O_3 FG square plates versus Winkler $(\overline{K}_w)$ and Pasternak $(\overline{K}_s)$ parameters. As can be seen from this figure, the dimensionless deflection diminishes when the foundation parameters increase. Compared to the Winkler parameter $(\overline{K}_w)$, the Pasternak foundation parameter $(\overline{K}_s)$ has more significant effect on decreasing the dimensionless deflection. Besides, the deflection computed by present quasi-3D theory are lower than those obtained from 2D theory which means the thickness stretching effect is more significant when the thickness of the plate is higher, but it is negligible with reducing the thickness of the plate. This indicates that the stretching effect is pronounced, and must be taken into account in the modelling of thick plate.

5. Conclusions

This study examines the bending response of FG plates resting on elastic foundations using a new developed 2D and quasi-3D shear strain theories. A new shear shape function that meets the boundary conditions with no tension or compression on the bottom and top surfaces of the plate is used in the theory, which only uses five unknowns, to account for a parabolic distribution of the transverse shear stress. Moreover, the shear correction factor has not been considered. The equilibrium equations were determined using the virtual work principle. In order to show the validity of the proposed theory, the analytical solutions of simply supported plates are produced using the double Fourier series and are compared to previously published solutions. The effects of a large number of parameters such as the

transverse normal strain, the form ratio of the plate, the length/thickness ratio, the volume fraction distributions, the various mixing laws as well as the boundary conditions on the deflection, axial displacements and the various stresses are examined in detail. The above-analyzed results allow for the following key conclusions:

- It is clear from all of the comparative experiments that the proposed theory exhibits strong agreement with the findings of previous 2D and quasi-3D HSDTs.
- Although there are five unknowns in the proposed quasi-3D HSDT, the results it produces are comparable to those of other published quasi-3D theories with more unknowns, such as the quasi-3D theories of Neves et al. (2012a, 2012b), which have nine unknowns, and Akavci and Tanrikulu (2015), which have six unknowns.
- The power law index affects how much a plate deflects. A material index number greater than 5 has very little impact.
- The thickness stretching effect was not taken into account, which resulted in the little disparity between the current 2D and quasi-3D shear deformation values.
- The findings show that the plate stiffens when the effects of normal deformations are taken into account, which reduces deflection and increases stresses.
- For thick plates, the thickness stretching effect is more pronounced, therefore it must be accounted in the modeling.

Finally, it can be concluded that the formulation developed here in can serve as a reference to future research and could be extended to the analysis of classical and thermal buckling of FG plates by introducing various combined boundary conditions.

Acknowledgment

The research reported herein was funded by the Deanship of Scientific Research at the University of Hail, Saudi Arabia, through the project number RG-21 084. The authors would like to express their deepest gratitude to the Deanship of Scientific Research and to the College of Engineering at the University of Hail for providing necessary support to conducting this research.

References

Abdelhak, Z., Hadji, L., Daouadji, T.H. and Adda Bedia, E.A. (2016), "Thermal buckling response of functionally graded sandwich plates with clamped boundary conditions", *Smart Struct. Syst. Int. J.*, **18**(2), 267–291. https://doi.org/10.12989/SSS.2016.18.2.267

Abdulrazzaq, M. A., Fenjan, R. M., Ahmed, R. A., & Faleh, N. M. (2020). "Thermal buckling of nonlocal clamped exponentially graded plate according to a secant function based refined theory". *Steel Compos., Struct.*, **35**(1), 147–157. https://doi.org/10.12989/SCS.2020.35.1.147

Akavci, S.S., Tanrikulu, A.H. (2015), "Static and free vibration analysis of functionally graded plates based on a new quasi-3D and 2D shear deformation theories",*Compos. Part B Eng.*, **83**(15),203-215.https://doi.org/10.1016/j.compositesb.2015.08.043.

Aldousari, S.M. (2017), "Bending analysis of different material distributions of functionally graded beam", *Appl. Phys. A.*, **123**(4),296.https://doi.org/10.1007/s00339-017-0854-0

Al Khateeb, S.A., Zenkour, A.M. (2014), "A refined four-unknown plate theory for advanced plates resting on elastic foundations in hygrothermal environment", *Compos. Struct.*, **111**, 240-248.https://doi.org/10.1016/j.compstruct.2013.12.033

Amar, H.H.L., Kaci, A., Houari, M.S.A., Bourada, A., Tounsi, A., Mahmoud, S.R. (2017), "A new simple three-unknown shear deformation theory for bending analysis of FG plates resting on elastic foundations", *Steel Compos. Struct. Int. J.*, **25**(6):717e26. https://doi.org/10.12989/scs.2017.25.6.717

Arefi, M., Allam, M.N.M. (2015), "Nonlinear responses of an arbitrary FGP circular plate resting on the Winkler-Pasternak foundation", *Smart Struct., Syst.*, **16**(1), 81-100. https://doi.org/10.12989/sss.2015.16.1.081

Barretta, R., Luciano F., Raimondo L., Francesco M.S., and Rosa P., (2016), "Functionally graded Timoshenko nanobeams: a novel nonlocal gradient formulation." *Composites Part B: Engineering* 100 208-219. https://doi.org/10.1016/j.compositesb.2016.05.052

Belkhodja, Y., Ouinas, D., Zaoui, F.Z., Fekirini, H. (2019), "A higher order exponential-trigonometric shear deformation theory for bending, vibration and buckling analysis of functionally graded material (FGM) plates: Part I", *Advanced Compos. Letters*, **28**, 1–19. https://doi.org/10.1177/0963693519875739

Belkhodja, Y., Ouinas, D., Fekirini, H. Viña Olay, J.A., Achour, B., Touahmia M. and Boukendakdji. M. (*2022*), "A new hybrid HSDT for bending, free vibration, and buckling analysis of FGM plates (2D & quasi-3D)", Smart Struct. Syst., **29**(3), 395-420. https://doi.org/10.12989/sss.2022.29.3.395.

Benyoucef, S., Mechab, I., Tounsi, A., Fekrar, A., Ait Atmane, H. and Adda, B.E.A. (2010), "Bending of thick functionally graded plates resting on Winkler–Pasternak elastic foundations",*Mech.Compos. Mater.*,**46**,425–434.https://doi.org/10.1007/s11029-010-9159-5

Carrera, E., Brischetto, S., Cinefra, M., Soave, M. (2011), "Effects of thickness stretching in functionally graded plates and shells", *Compos. Part B Eng.*, **42**(2),123-133.https://doi.org/10.1016 /j.compositesb. 2010.10.005

Demirhan, P.A., Taskin, V., (2019). "Bending and free vibration analysis of Levy-type porous functionally graded plate using state space approach", *Compos. B Eng.*, **160**, 661–676. http://dx.doi.org/10.1016/j.compositesb.2018.12.020 .

Grover, N., Maiti, D., Singh, B. (2013), "A new inverse hyperbolic shear deformation theory for static and buckling analysis of laminated composite and sandwich plates". *Compos. Struct.*,**95**,667-675. https://doi.org/10.1016/j.compstruct.2012.08.012

Guerroudj, H. Z., Yeghnem, R., Kaci, A., Zaoui, F. Z., Benyoucef, S. and Tounsi, A. (2018). "Eigen-frequencies of advanced composite plates using an efficient hybrid quasi-3D shear deformation theory". *Smart Struct. Syst. Int. J.*,**22**(1), 121–132. https://doi.org/10.12989/SSS.2018.22.1.121

Hebbar, N., Hebbar, I., Ouinas D. and Bourada, M. (2020), "Numerical modeling of bending, buckling, and vibration of functionally graded beams by using a higher-order shear deformation theory", *Frattura ed Integrità Strutturale*, **14**(52), 230-246. https://doi.org/10.3221/IGF-ESIS.52.18

Hosseini-Hashemi, S.H., Fadaee, M. and Atashipour, S.R. (2011), "Study on the free vibration of thick functionally graded rectangular plates according to a new exact closed form procedure", *Compos.Struct.*, **93**(2),722-735.https://doi.org/10.1016/j.compstruct.2010.08.007

Jha, D.K., Kant, T. and Singh, R.K. (2013), "Free vibration response of functionally graded thick plates with shear and normal deformations effects", *Compos. Struct.*, **96**,799-823. https://doi.org/ 10.1016/j.compstruct.2012.09.034

Le, C.I., Pham, V.N., and Nguyen, D.K. (2020). "Free vibration of FGSW plates partially supported by Pasternak foundation based on refined shear deformation theories", *Mathematical Problems in Engineering*, **2020**, 7180453. https://doi.org/10.1155/2020/7180453

Lee, W.H., Han, S.C. and Park, W.T. (2015), "A refined higher order shear and normal deformation theory for E-, P-, and S-FGM plates on Pasternak elastic foundation", *Compos. Struct.*, **122**,330-342.https://doi.org/10.1016/j.compstruct.2014.11.047

Mahmoudi, A., Benyoucef, S., Tounsi, A., Benachour, A. and Adda, B.EA. (2018), "On the effect of the micromechanical models on the free vibration of rectangular FGM plate resting on elastic foundation", *Earthquakes & Structures Int. J.*, **14**(2),117-128.https://doi.org/10. 12989/eas.2018.14.2.117

Mantari, J.L. and Granados, E.V. (2016), "An original FSDT to study advanced composites on elastic foundation", *Thin-Walled Structures*, **107**, 80-89. https://doi.org/10.1016/j.tws.2016.05.024

Mantari, J.L., Granados, E.V., Hinostroza, M.A., Guedes Soares, C., (2014). "Modelling advanced composite plates resting on elastic foundation by using a quasi-3D hybrid type HSDT", *Compos. Struct.*, **118**, 455–471. https://doi.org/10.1016/j. compstruct.2014.07.039 .

Mantari, J.L. and Soares, C.G. (2013), "A novel higher-order shear deformation theory with stretching effect for functionally graded plates", *Compos. Part B Eng.*, **45**(1), 2682-2681.https://doi.org/ 10.1016/j.compositesb.2012.05.036

Mantari, J.L., Soares, C.G. (2015). "Five-unknowns generalized hybrid-type quasi- 3D HSDT for advanced composite plates", *Appl. Math. Model.*, **39** (18), 5598–5615. https://doi.org/10.1016/j.apm.2015.01.020 .

Meftah, A., Bakora, A., Zaoui, F. Z., Tounsi, A. and Bedia, E. A. A. (2017), "A non-polynomial four variable refined plate theory for free vibration of functionally graded thick rectangular plates on elastic foundation", *Steel Compos. Struct. Int. J.*,**23**(3), 317–330. https://doi.org/10.12989/SCS. 2017.23.3.317

Mengzhen, L., Renjun Y., Guedes, C.S. (2021), "Free vibration of advanced composite plates using a new higher order shear deformation theory", *European Journal of Mechanics / A Solids*, **88** , 104236. https://doi.org/10.1016/j.euromechsol.2021.104236

Meradjah, M., Bouakkaz, K., Zaoui, F. Z. and Tounsi, A. (2018), "A refined quasi-3D hybrid-type higher order shear deformation theory for bending and Free vibration analysis of advanced composites beams", *Wind and Structures*, **27**(4), 269–282. https://doi.org/10.12989/WAS. 2018.27.4.269

Mori, T. and Tanaka, K. (1973), "Average Stress in Matrix and Average Elastic Energy of Materials with Misfitting Inclusions", *Acta Metallurgica*,**21**(5), 571-574. http://dx.doi.org/10.1016/0001-6160 (73)90064-3

Neves, A.M.A., Ferreira, A.J.M., Carrera, E., Roque, C.M.C., Cinefra, M., Jorge, R.M.N. and Soares, C.M.M. (2012a), "A quasi-3D sinusoidal shear deformation theory for the static and free vibration analysis of functionally graded plates", *Compos. Part B Eng.*, 43(2), 711-725. https://doi.org/10.1016/j.compositesb.2011.08.009

Neves, A.M.A., Ferreira, A.J.M., Carrera, E., Cinefra, M., Roque, C.M.C., Jorge, R.M.N. and Soares, C.M.M. (2012b), "A quasi-3D hyperbolic shear deformation theory for the static and free vibration analysis of functionally graded plates", *Compos. Struct.*, **94**(5), 1814-1825. https://doi.org/10.1016/j.compstruct.2011.12.005

Nguyen, T.K. (2015), "A higher-order hyperbolic shear deformation plate model for analysis of functionally graded materials", *Int. J. Mech. Mater. Des.*, **11**(2), 203-219.https://doi.org/10.1007/s10999-014-9260-3

Ouinas, D., Achour, B. (2013), "Buckling analysis of laminated composite plates [(θ/-θ)] containing an elliptical notch", *Compos. Part B Eng*., **55**, 575-579. https://doi.org/10.1016/j.compositesb.2013.07.011

Rachid, A., Ouinas, D., Lousdad, A., Zaoui, F.Z., Achour, B., Gasmi, H., Butt, T.A., Tounsi, A. (2022), **"**Mechanical behavior and free vibration analysis of FG doubly curved shells on elastic foundation via a new modified displacements field model of 2D and Quasi-3D HSDTs", *Thin-Walled Struct*., **172**, 108783. https://doi.org/10.1016/j.tws.2021.10878

Sidhoum, I.A., Boutchicha, D., Benyoucef, S. and Tounsi, A. (2018), "An original HSDT for free vibration analysis of functionally graded plates", *Steel Compos. Struct. Int. J.*, **25**(6),735-745.https://doi.org/10.12989/scs.2017.25.6.735

Thai, H.T., Kim, S.E. (2013), "A simple higher-order shear deformation theory for bending and free vibration analysis of functionally graded plates", *Compos. Struct*., **96**, 165–173. https://doi.org/10.1016/j.compstruct.2012.08.025

Thai, H.T., Park, M. and Choi, D.H. (2013), "A simple refined theory for bending, buckling, and vibration of thick plates resting on elastic foundation", *Int. J. Mech. Sci.*, **73**,40–52.https://doi.org/10.1016/j.ijmecsci.2013.03.017.

Vaghefi, R., Baradaran, G.H. and Koohkan, H. (2010), "Three-dimensional static analysis of thick functionally graded plates by using meshless local Petrov–Galerkin (MLPG) method", *Eng. Anal.Bound. Elem.*, **34**,564-573. https://doi.org/10.1016/j.enganabound.2010.01.005

Vu, T.-V., Khosravifard, A., Hematiyan, M.R., Bui, T.Q., (2019), "Enhanced meshfree method with new correlation functions for functionally graded plates using a refined inverse sin shear deformation plate theory", *Eur. J. Mech. Solid*., **74**, 160–175. https://doi.org/10.1016/j.euromechsol.2018.11.005

Xiang, S., Kang, G. (2013), "A nth-order shear deformation theory for the bending analysis on the functionally graded plates", *Eur. J. Mech. Solid.*, **37**, 336–343. https://doi.org/10.1016/j.euromechsol.2012.08.005

Yarasca, J., Mantari, J.L. And Arciniega, R.A. (2016), "Hermite–Lagrangian finite element formulation to study functionally graded sandwich beams", *Compos. Struct*., **140**:567-581.https://doi.org/10.1016/j.compstruct.2016.01.015

Younsi, A., Tounsi, A., Zaoui, F. Z., Bousahla, A. A. and Mahmoud, S. R. (2018), "Novel quasi-3D and 2D shear deformation theories for bending and free vibration analysis of FGM plates", *Geomechanics & Engineering Int. J.*,**14**(6), 519–532. https://doi.org/10.12989/GAE.2018.14.6.519

Zaoui, F.Z., Hanifi, H.A.L., Younsi, A., Meradjah, M., Tounsi, A. and Ouinas, D. (2017b),"Free vibration analysis of functionally graded beams using a higher-order shear deformation theory". *Math. Model. Eng. Probl.*,**4**(1),7-12.https://doi.org/10.18280/mmep.040102

Zaoui, F.Z., Ouinas, D., B., Achour, M., Touhamia, M., Boukendakdji, R.L., Enamur, A., Alawi., Viña Olay, J.A. (2022b), "Mathematical Approach for Mechanical Behaviour Analysis of FGM Plates on Elastic Foundation". *Mathematics*, **10**, 4764. https://doi.org/10.3390/math10244764

Zaoui, F.Z., Ouinas, D., Achour, B., Tounsi, A., Latifee, E.R., Al-Naghi, A.A.A. (2022a), "A hyperbolic shear deformation theory for natural frequencies study of functionally graded plates on elastic supports". *J. Compos. Sci.*, **6**(10), 285. https://doi.org/10.3390/jcs6100285

Zaoui, F.Z., Ouinas, D., Tounsi, A. (2019), "New 2D and quasi-3D shear deformation theories for free vibration of functionally graded plates on elastic foundations", *Compos. Part B Eng.*, **159**,231-347.https://doi.org/10.1016/j.compositesb.2018.09.051

Zaoui, F.Z., Ouinas, D., Tounsi, A. Viña Olay, J.A., Achour B., Touahmia M. (2021),"Fundamental frequency analysis of functionally graded plates with temperature-dependent properties based on improved exponential-trigonometric two-dimensional higher shear deformation theory", *Archive of Applied Mechanics*, **91**(3), 859–881. https://doi.org/10.1007/s00419-020-01793-1

Zaoui, F.Z., Tounsi, A. and Ouinas, D. (2017a), "Free vibration of functionally graded plates resting on elastic foundations based on quasi-3D hybrid-type higher order shear deformation theory", *Smart Struct. Syst. Int. J.*,**20**(4), 509-524.https://doi.org/10.12989/sss.2017.20.4.509

Zaoui, F.Z., Tounsi, A. Ouinas, D., Viña Olay, J.A. (2020), "A refined HSDT for bending and dynamic analysis of FGM plates", *Struct. Eng. Mech. Int.J.*,**74**(1), 105-119. http://dx.doi.org/ 10. 12989/ sem. 2020.74.1.105
Zhang, H., Jiang, J.K. and Zhang, Z.C. (2014), "Three-dimensional elasticity solutions for bending of generally supported thick functionally graded plates", *Appl. Math. Mech.*,**35**(11),1467-1478. https://doi.org/10.1007/s10483-014-1871-7

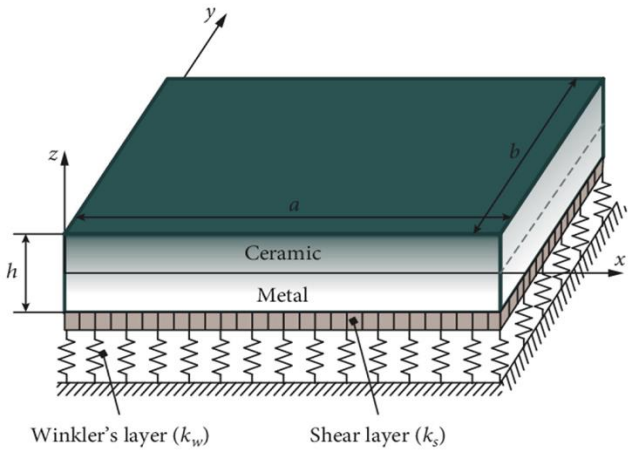

Fig. 1 Geometry and coordinates of the considered FGM plate on elastic foundation.

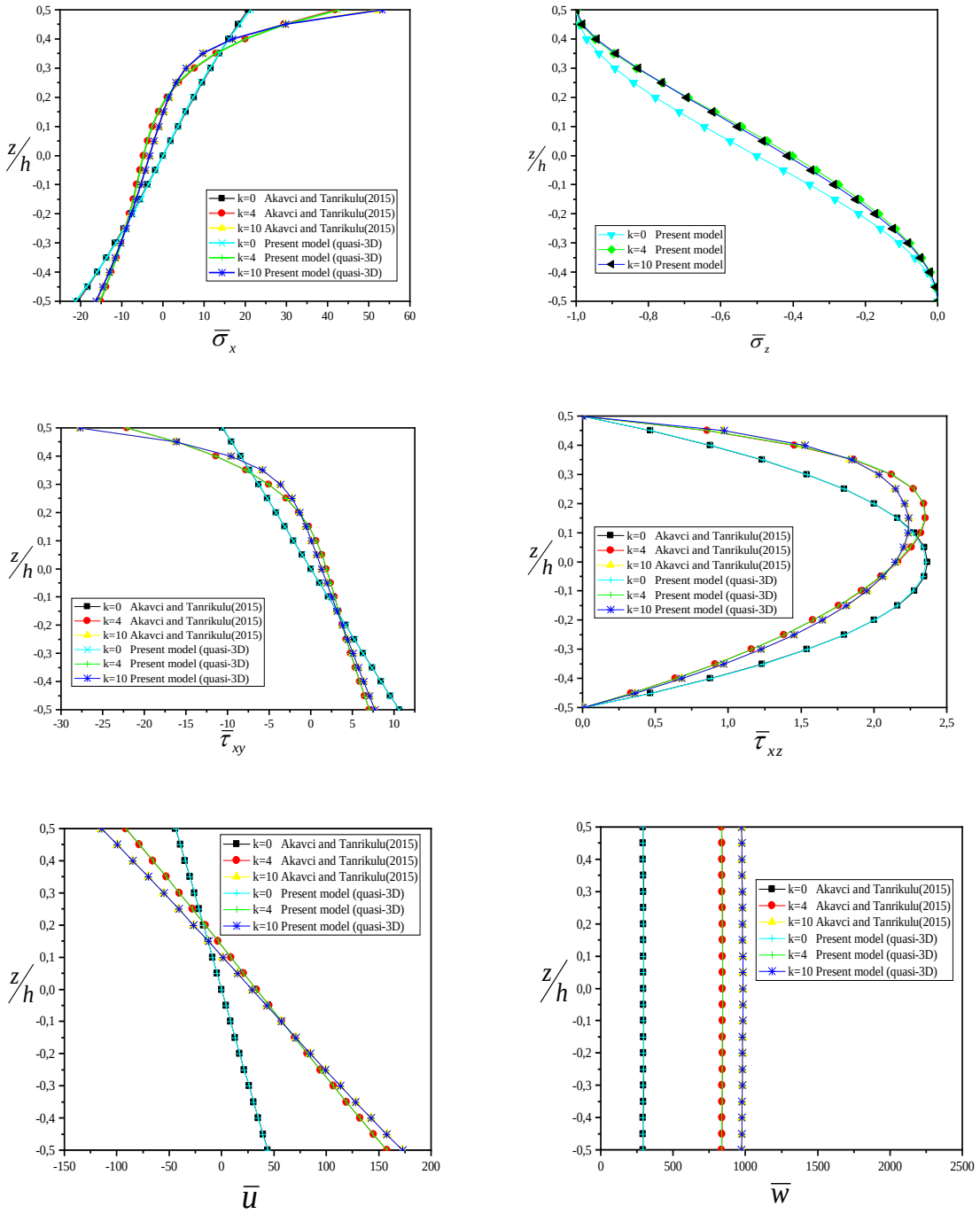

Fig. 2 Distributions of the non-dimensional displacements and stresses through the thickness of square P-FGM plate ($a/h=10$)

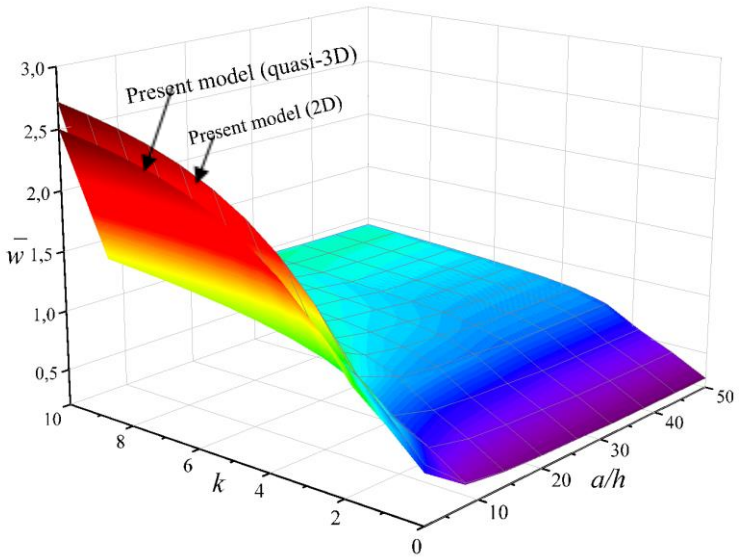

Fig. 3 Effect of the power-law index k and side-to-thickness ratio a/h on the non-dimensional deflection $\overline{w}$ of simply supported Al/Al_2O_3 P-FGM plates.

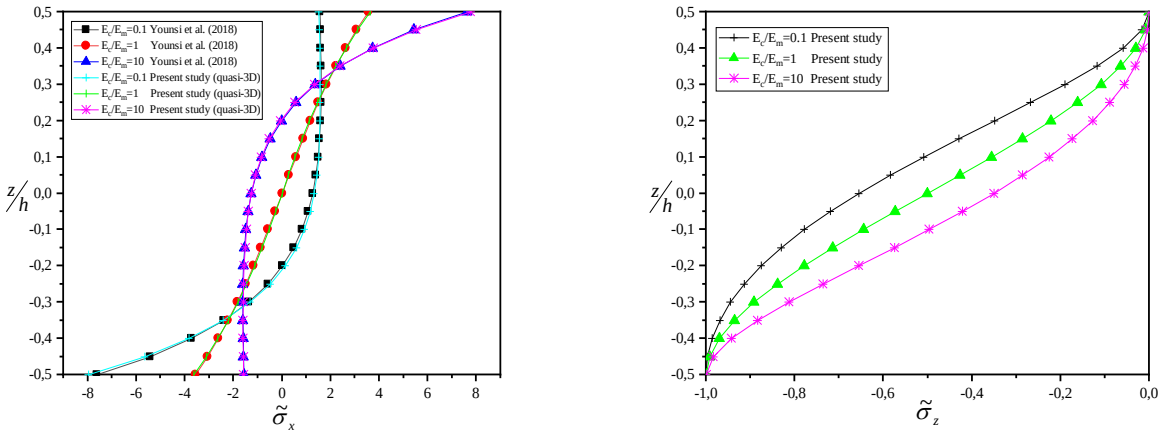

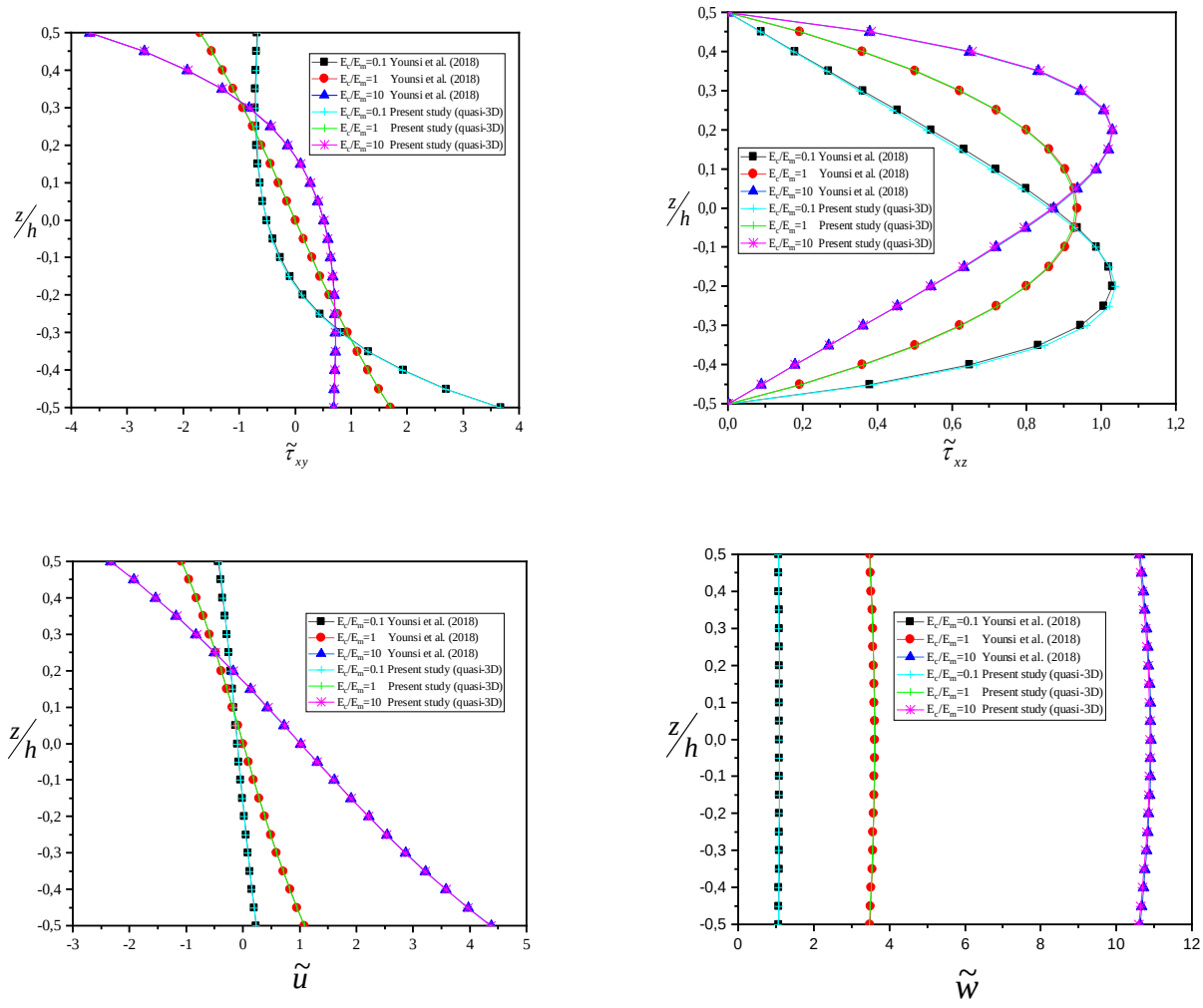

Fig. 4 Distributions of the non-dimensional displacements and stresses through the thickness of square E-FGM plate ($a/h=10$)

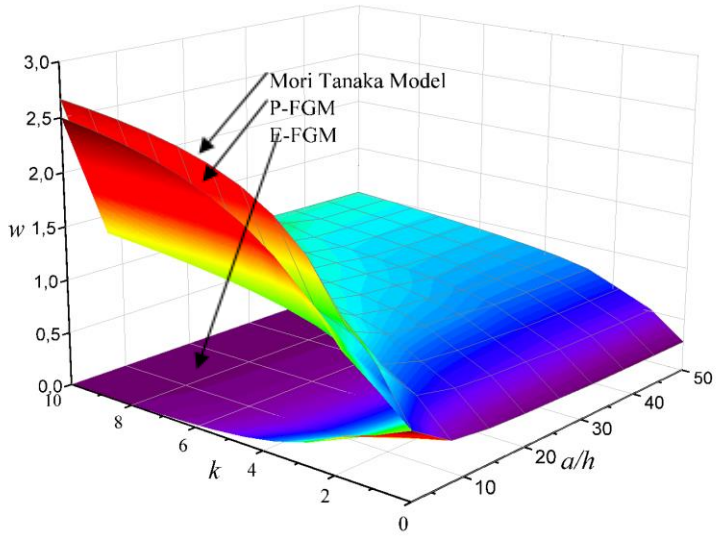

Fig.5 Non-dimensional deflection variation $\overline{w}$ of different models of FG plates for various values of power-law index k and side-to-thickness ratio (a/h).

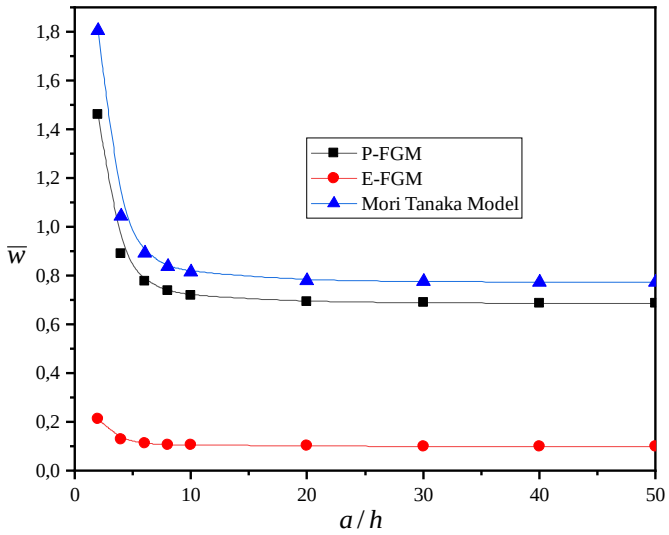

Fig.6 Effect of the side-to-thickness ratio (a/h) on the non-dimensional deflection of different FG plates.

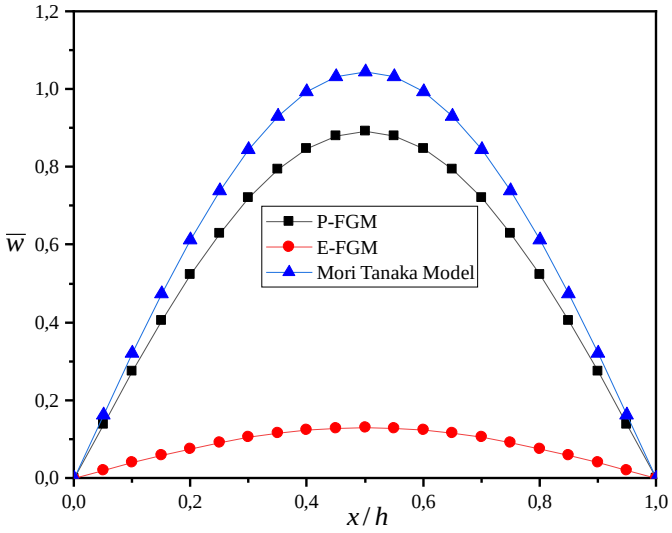

Fig. 7 Comparison of the deflection of Mori-Tanaka model, P-FGM and E-FGM plates $(a/h=4,\ k=2)$.

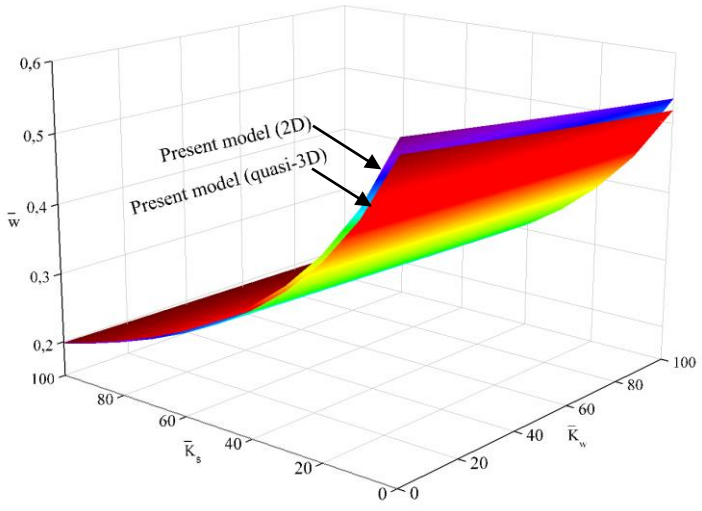

Fig.8 Effect of foundation parameters $(\overline{K}_w, \overline{K}_s)$ on the non-dimensional deflection $\overline{w}$ of FG square plates under sinusoidal load $(k=1,\ a/h=10)$.

Table 1 Material properties used in the FG plates.

Material	Properties		
	$E(GPa)$	ν	ρ (kg/m^3)
Aluminum (Al)	70	0.3	2702
Alumina (Al_2O_3)	380	0.3	3800
Zirconia (ZrO_2)	200	0.3	5700

Table 2 The non-dimensional displacement and stress components of an Al/Al_2O_3 FG square plate subjected to uniformly distributed load ($a/h=10$).

k	Theory	ε_z	$\bar{w}(0)$	$\bar{\sigma}_x\left(\frac{h}{2}\right)$	$\bar{\sigma}_y\left(\frac{h}{3}\right)$	$\bar{\tau}_{xz}(0)$	$\bar{\tau}_{yz}\left(\frac{h}{6}\right)$	$\bar{\tau}_{xy}\left(-\frac{h}{3}\right)$
0	Akavci and Tanrikulu (2015)	= 0	0.4665	2.8909	1.9103	0.4988	0.4363	1.2857
	Akavci and Tanrikulu (2015)	≠ 0	0.4635	2.9981	1.8925	0.4782	0.4315	1.2578
	Younsi et al. (2018)	= 0	0.4665	2.8913	1.9102	0.5043	0.4367	1.2855
	Younsi et al. (2018)	≠ 0	0.4637	2.9919	1.8932	0.5042	0.4317	1.2585
	Present study	= 0	0.4665	2.8912	1.9102	0.5043	0.4369	1.2856
	Present study	≠ 0	0.4625	3.0729	1.8756	0.4761	0.4307	1.2548
1	Akavci and Tanrikulu (2015)	= 0	0.9288	4.4707	2.1693	0.4988	0.5364	1.1141
	Akavci and Tanrikulu (2015)	≠ 0	0.8977	4.6110	2.0822	0.4782	0.5119	1.0211
	Younsi et al. (2018)	= 0	0.9287	4.4713	2.1692	0.5043	0.5370	1.1141
	Younsi et al. (2018)	≠ 0	0.8980	4.6005	2.0832	0.4791	0.5121	1.0225
	Present study	= 0	0.9287	4.4713	2.1692	0.5042	0.5372	1.1141
	Present study	≠ 0	0.8961	4.7379	2.0578	0.4761	0.5114	1.0206
2	Akavci and Tanrikulu (2015)	= 0	1.1940	5.2248	2.0342	0.4581	0.5643	0.9909
	Akavci and Tanrikulu (2015)	≠ 0	1.1376	5.3825	1.9257	0.4524	0.5081	0.8921
	Younsi et al. (2018)	= 0	1.1940	5.2256	2.0340	0.4637	0.5657	0.9908
	Younsi et al. (2018)	≠ 0	1.1380	5.3726	1.9281	0.4532	0.5082	0.8926
	Present study	= 0	1.1940	5.2255	2.0340	0.4636	0.5658	0.9908
	Present study	≠ 0	1.1352	5.5232	1.8972	0.4505	0.5074	0.8902
4	Akavci and Tanrikulu (2015)	= 0	1.3888	5.8855	1.7205	0.4090	0.5253	1.0305
	Akavci and Tanrikulu (2015)	≠ 0	1.3259	6.0382	1.6062	0.4358	0.4804	0.9274
	Younsi et al. (2018)	= 0	1.3890	5.8866	1.7202	0.4151	0.5278	1.0303
	Younsi et al. (2018)	≠ 0	1.3262	6.0301	1.6101	0.4365	0.4806	0.9279
	Present study	= 0	1.3889	5.8865	1.7202	0.4149	0.5279	1.0303
	Present study	≠ 0	1.3237	6.1920	1.5744	0.4341	0.4797	0.9256
10	Akavci and Tanrikulu (2015)	= 0	1.5875	7.3617	1.2828	0.4436	0.4159	1.0705
	Akavci and Tanrikulu (2015)	≠ 0	1.5453	7.5123	1.2016	0.4332	0.4561	0.9860
	Younsi et al. (2018)	= 0	1.5875	7.3628	1.2825	0.4495	0.4174	1.0703
	Younsi et al. (2018)	≠ 0	1.5454	7.5064	1.2059	0.4339	0.4562	0.9862
	Present study	= 0	1.5875	7.3628	1.2825	0.4495	0.4176	1.0703
	Present study	≠ 0	1.5436	7.6914	1.1724	0.4314	0.4554	0.9852

Table 3 Non-dimensional displacement and stress of an Al/Al_2O_3 FG square plate subjected to sinusoidal load.

k	Theory	ε_z	$\bar{\sigma}_x(h/3)$			$\bar{w}(0)$		
			$a/h=4$	$a/h=10$	$a/h=100$	$a/h=4$	$a/h=10$	$a/h=100$
1	Carrera et al. (2011)	$\neq 0$	0.6221	1.5064	14.9690	0.7171	0.5875	0.5625
	Neves et al. (2012a)	$\neq 0$	0.5925	1.4945	14.9690	0.6997	0.5845	0.5624
	Neves et al. (2012b)	$\neq 0$	0.5910	1.4917	14.9440	0.7020	0.5868	0.5648
	Hebali et al. (2014)	$\neq 0$	0.5952	1.4954	14.9630	0.6910	0.5686	0.5452
	Akavci and Tanrikulu (2015)	= 0	0.5806	1.4895	14.9670	0.7282	0.5889	0.5625
	Akavci and Tanrikulu (2015)	$\neq 0$	0.5754	1.4322	14.3060	0.6908	0.5691	0.5457
	Younsi et al. (2018)	= 0	0.5808	1.4896	14.9675	0.7283	0.5889	0.5625
	Younsi et al. (2018)	$\neq 0$	0.5758	1.4330	14.3135	0.6910	0.5692	0.5459
	Present study	= 0	0.5803	1.4894	14.9675	0.7280	0.5889	0.5625
	Present study	$\neq 0$	0.5705	1.4157	14.1330	0.6896	0.5680	0.5447
4	Carrera et al. (2011)	$\neq 0$	0.4877	1.1971	11.9230	1.1585	0.8821	0.8286
	Neves et al. (2012a)	$\neq 0$	0.4404	1.1783	11.9320	1.1178	0.8750	0.8286
	Neves et al. (2012b)	$\neq 0$	0.4340	1.1593	11.7380	1.1095	0.8698	0.8241
	Hebali et al. (2014)	$\neq 0$	0.4507	1.1779	11.8710	1.0964	0.8413	0.7926
	Akavci and Tanrikulu (2015)	= 0	0.4431	1.1787	11.9200	1.1613	0.8818	0.8287
	Akavci and Tanrikulu (2015)	$\neq 0$	0.4247	1.1017	11.0880	1.0983	0.8417	0.7925
	Younsi et al. (2018)	= 0	0.4437	1.1789	11.9209	1.1609	0.8817	0.8287
	Younsi et al. (2018)	$\neq 0$	0.4260	1.1045	11.1152	1.0982	0.8419	0.7928
	Present study	= 0	0.4424	1.1783	11.9208	1.1618	0.8818	0.8287
	Present study	$\neq 0$	0.4181	1.0802	10.8633	1.0970	0.8403	0.7910
10	Carrera et al. (2011)	$\neq 0$	0.3965	0.8965	8.9077	1.3745	1.0072	0.9361
	Neves et al. (2012a)	$\neq 0$	0.3227	1.1783	11.9320	1.3490	0.8750	0.8286
	Neves et al. (2012b)	$\neq 0$	0.3108	0.8467	8.6013	1.3327	0.9886	0.9228
	Hebali et al. (2014)	$\neq 0$	0.3325	0.8889	8.9977	1.3333	0.9791	0.9114
	Akavci and Tanrikulu (2015)	= 0	0.3242	0.8778	8.9059	1.3917	1.0089	0.9362
	Akavci and Tanrikulu (2015)	$\neq 0$	0.3095	0.8229	8.3185	1.3352	0.9818	0.9141
	Younsi et al. (2018)	= 0	0.3248	0.8780	8.9059	1.3915	1.0088	0.9362
	Younsi et al. (2018)	$\neq 0$	0.3109	0.8259	8.3473	1.3353	0.9819	0.9141
	Present study	= 0	0.3235	0.8775	8.9059	1.3917	1.0089	0.9362
	Present study	$\neq 0$	0.3033	0.8031	8.1118	1.3333	0.9807	0.9130

Table 4 Non-dimensional deflection $\bar{w}(0)=\frac{10h^3E_0}{a^4q_0}w\left(\frac{a}{2},\frac{b}{2},0\right)$ of E-FGM plates subjected to sinusoidal distributed load ($a/h=2$).

b/a	Theory	ε_z	k					
			0.1	0.3	0.5	0.7	1	1.5
1	Zenkour (2007)	≠ 0	0.5769	0.5247	0.4766	0.4324	0.3726	0.2890
	Zenkour (2007)	= 0	0.5730	0.5180	0.4678	0.4221	0.3611	0.2771
	Mantari and Soares (2016)	≠ 0	0.5778	0.5224	0.4717	0.4256	0.3648	0.2793
	Mantari and Soares (2016)	= 0	0.6362	0.5751	0.5194	0.4687	0.4017	0.3079
	Akavci and Tanrikulu (2015)	= 0	0.6351	0.5741	0.5185	0.4679	0.4004	0.3075
	Akavci and Tanrikulu (2015)	≠ 0	0.5750	0.5198	0.4694	0.4236	0.3624	0.2780
	Younsi et al. (2018)	= 0	0.6355	0.5745	0.5189	0.4683	0.4007	0.3077
	Younsi et al. (2018)	≠ 0	0.5758	0.5205	0.4701	0.4242	0.3629	0.2784
	Present study	= 0	0.6343	0.5734	0.5179	0.4674	0.4000	0.3072
	Present study	≠ 0	0.5731	0.5181	0.4679	0.4222	0.3612	0.2771
2	Zenkour (2007)	≠ 0	1.1944	1.0859	0.9864	0.8952	0.7726	0.6017
	Zenkour (2007)	= 0	1.1879	1.0739	0.9700	0.8754	0.7493	0.5757
	Mantari and Soares (2016)	≠ 0	1.1940	1.0794	0.9750	0.8799	0.7537	0.5786
	Mantari and Soares (2016)	= 0	1.2776	1.1553	1.0441	0.9430	0.8092	0.6237
	Akavci and Tanrikulu (2015)	= 0	1.2763	1.1541	1.0431	0.9422	0.8079	0.6234
	Akavci and Tanrikulu (2015)	≠ 0	1.1938	1.0765	0.9723	0.8775	0.7511	0.5771
	Younsi et al. (2018)	= 0	1.2768	1.1546	1.0435	0.9426	0.8082	0.6236
	Younsi et al. (2018)	≠ 0	1.1917	1.0774	0.9731	0.8782	0.7517	0.5775
	Present study	= 0	1.2753	1.1532	1.0423	0.9415	0.8074	0.6231
	Present study	≠ 0	1.1880	1.0740	0.9701	0.8755	0.7494	0.5758
3	Zenkour (2007)	≠ 0	1.4429	1.3116	1.9112	1.0811	0.9333	0.7275
	Zenkour (2007)	= 0	1.4354	1.2977	1.1722	1.0579	0.9056	0.6961
	Mantari and Soares (2016)	≠ 0	1.4421	1.3037	1.1776	1.0627	0.9104	0.6992
	Mantari and Soares (2016)	= 0	1.5340	1.3873	1.2540	1.1329	0.9725	0.7506
	Akavci and Tanrikulu (2015)	= 0	1.5327	1.3861	1.2530	1.1320	0.9712	0.7503
	Akavci and Tanrikulu (2015)	≠ 0	1.4386	1.3005	1.1748	1.0602	0.9076	0.6976
	Younsi et al. (2018)	= 0	1.5332	1.3866	1.2534	1.1324	0.9715	0.7504
	Younsi et al. (2018)	≠ 0	1.4396	1.3015	1.1756	1.0610	0.9082	0.6981
	Present study	= 0	1.5316	1.3852	1.2521	1.1313	0.9706	0.7499
	Present study	≠ 0	1.4354	1.2977	1.1722	1.0579	0.9057	0.6961

Table 5 Non-dimensional stress $\bar{\sigma}_x\left(\frac{h}{2}\right)=\frac{h^2}{a^2 q_0}\sigma_x\left(\frac{a}{2},\frac{b}{2},\frac{h}{2}\right)$ of E-FGM plates subjected to sinusoidal distributed load ($a/h=10$).

b/a	Theory	ε_z	k								
			0.1	0.3	0.5	0.7	1	1.5	2	2.5	3
1	Mantari and Soares (2016)	$\neq 0$	0.2196	0.2345	0.2503	0.2671	0.2944	0.3460	0.4065	0.4775	0.5603
	Mantari and Soares (2016)	= 0	0.2062	0.2204	0.2355	0.2515	0.2774	0.3264	0.3835	0.4502	0.5278
	Akavci and Tanrikulu (2015)	= 0	0.2063	0.2205	0.2356	0.2516	0.2776	0.3266	0.3838	0.4504	0.5281
	Akavci and Tanrikulu (2015)	$\neq 0$	0.2142	0.2285	0.2438	0.2601	0.2866	0.3370	0.3964	0.4664	0.5485
	Younsi et al. (2018)	= 0	0.2063	0.2205	0.2355	0.2516	0.2775	0.3265	0.3837	0.4504	0.5279
	Younsi et al. (2018)	$\neq 0$	0.2137	0.2280	0.2433	0.2595	0.2860	0.3363	0.3957	0.4657	0.5478
	Present study	= 0	0.2063	0.2205	0.2356	0.2517	0.2776	0.3266	0.3838	0.4505	0.5282
	Present study	$\neq 0$	0.2195	0.2344	0.2502	0.2670	0.2943	0.4359	0.4064	0.4773	0.5602
2	Mantari and Soares (2016)	$\neq 0$	0.4552	0.4867	0.5200	0.5554	0.6126	0.7201	0.8449	0.9898	1.1580
	Mantari and Soares (2016)	= 0	0.4350	0.4649	0.4966	0.5303	0.5850	0.6881	0.8085	0.9490	1.1125
	Akavci and Tanrikulu (2015)	= 0	0.4351	0.4650	0.4968	0.5305	0.5852	0.6884	0.8088	0.9493	1.1129
	Akavci and Tanrikulu (2015)	$\neq 0$	0.4466	0.4773	0.5098	0.5443	0.6002	0.7058	0.8289	0.9725	1.1397
	Younsi et al. (2018)	= 0	0.4351	0.4650	0.4967	0.5305	0.5851	0.6883	0.8087	0.9492	1.1128
	Younsi et al. (2018)	$\neq 0$	0.4459	0.4765	0.5090	0.5435	0.5993	0.7048	0.8278	0.8278	1.1388
	Present study	= 0	0.4351	0.4650	0.4968	0.5306	0.5852	0.6884	0.8089	0.9494	1.1131
	Present study	$\neq 0$	0.4551	0.4865	0.5199	0.5553	0.6124	0.7199	0.8447	0.9897	1.1579
3	Mantari and Soares (2016)	$\neq 0$	0.5514	0.5896	0.6302	0.6733	0.7427	0.8730	1.0240	1.1990	1.4017
	Mantari and Soares (2016)	= 0	0.5288	0.5651	0.6037	0.6447	0.7112	0.8365	0.9828	1.1536	1.3523
	Akavci and Tanrikulu (2015)	= 0	0.5290	0.5653	0.6039	0.6449	0.7114	0.8368	0.9832	1.1540	1.3528
	Akavci and Tanrikulu (2015)	$\neq 0$	0.5418	0.5791	0.6187	0.6608	0.7289	0.8570	1.0061	1.1797	1.3813
	Younsi et al. (2018)	= 0	0.5289	0.5652	0.6038	0.6449	0.7113	0.8367	0.9831	1.1538	1.3527
	Younsi et al. (2018)	$\neq 0$	0.5410	0.5783	0.6179	0.6599	0.7279	0.8559	1.0050	1.1786	1.3803
	Present study	= 0	0.5290	0.5653	0.6039	0.6450	0.7114	0.8368	0.9833	1.1541	1.3529
	Present study	$\neq 0$	0.5512	0.5895	0.6300	0.6731	0.7425	0.8728	1.0238	1.1988	1.4016

Table 6 Non-dimensional stress $\bar{\tau}_{xz}(0)=\frac{h}{a q_0}\tau_{xz}\left(0,\frac{b}{2},0\right)$ of E-FGM plates subjected to sinusoidal distributed load ($a/h=10$).

b/a	Theory	ε_z	k								
			0.1	0.3	0.5	0.7	1	1.5	2	2.5	3
1	Mantari and Soares (2016)	$\neq 0$	0.2454	0.2450	0.2442	0.2430	0.2405	0.2344	0.2263	0.2162	0.2045
	Mantari and	= 0	0.2380	0.2376	0.2368	0.2356	0.2330	0.2268	0.2185	0.2094	0.1985

	Soares (2016)										
	Akavci and Tanrikulu (2015)	= 0	0.2434	0.2430	0.2422	0.2410	0.2385	0.2324	0.2242	0.2140	0.2023
	Akavci and Tanrikulu (2015)	≠ 0	0.2367	0.2364	0.2359	0.2353	0.2338	0.2300	0.2249	0.2182	0.2102
	Younsi et al. (2018)	= 0	0.2416	0.2412	0.2404	0.2392	0.2366	0.2305	0.2222	0.2121	0.2003
	Younsi et al. (2018)	≠ 0	0.2371	0.2369	0.2364	0.2357	0.2342	0.2304	0.2252	0.2186	0.2105
	Present study	= 0	0.2461	0.2457	0.2449	0.2437	0.2412	0.2351	0.2269	0.2168	0.2051
	Present study	≠ 0	0.2357	0.2354	0.2350	0.2343	0.2328	0.2291	0.2240	0.2174	0.2094
2	Mantari and Soares (2016)	≠ 0	0.3927	0.3921	0.3908	0.3889	0.3849	0.3752	0.3621	0.3460	0.3273
	Mantari and Soares (2016)	= 0	0.3810	0.3803	0.3790	0.3770	0.3730	0.3630	0.3497	0.3344	0.3165
	Akavci and Tanrikulu (2015)	= 0	0.3896	0.3889	0.3877	0.3857	0.3817	0.3719	0.3588	0.3425	0.3237
	Akavci and Tanrikulu (2015)	≠ 0	0.3790	0.3787	0.3779	0.3768	0.3744	0.3684	0.3602	0.3496	0.3368
	Younsi et al. (2018)	= 0	0.3867	0.3860	0.3847	0.3828	0.3787	0.3689	0.3557	0.3394	0.3206
	Younsi et al. (2018)	≠ 0	0.3797	0.3793	0.3786	0.3774	0.3750	0.3691	0.3608	0.3501	0.3373
	Present study	= 0	0.3939	0.3933	0.3920	0.3901	0.3860	0.3763	0.3632	0.3470	0.3282
	Present study	≠ 0	0.3774	0.3770	0.3763	0.3752	0.3728	0.3669	0.3587	0.3482	0.3355
3	Mantari and Soares (2016)	≠ 0	0.4418	0.4411	0.4396	0.4375	0.4330	0.4221	0.4074	0.3893	0.3683
	Mantari and Soares (2016)	= 0	0.4286	0.4279	0.4264	0.4242	0.4196	0.4084	0.3934	0.3761	0.3558
	Akavci and Tanrikulu (2015)	= 0	0.4383	0.4376	0.4361	0.4340	0.4294	0.4185	0.4036	0.3854	0.3642
	Akavci and Tanrikulu (2015)	≠ 0	0.4265	0.4261	0.4252	0.4239	0.4212	0.4146	0.4053	0.3934	0.3789
	Younsi et al. (2018)	= 0	0.4350	0.4343	0.4328	0.4307	0.4261	0.4151	0.4002	0.3819	0.3607
	Younsi et al. (2018)	≠ 0	0.4273	0.4268	0.4260	0.4247	0.4220	0.4153	0.4059	0.3940	0.3795
	Present study	= 0	0.4432	0.4425	0.4410	0.4389	0.4343	0.4234	0.4086	0.3904	0.3693
	Present study	≠ 0	0.4246	0.4242	0.4234	0.4221	0.4194	0.4128	0.4036	0.3918	0.3775

Table 7 Non-dimensional central displacement $\bar{w}(0) = G(h)w / hq_0$ and in-plane normal stress $\bar{\sigma}_x(0) = \sigma_x(0)/q_0$ of E-FGM plates subjected to uniformly distributed load.

h/a	Quantity	Theory	E_0 / E_1				
			0.1	0.5	1	2	10
0.2	$\bar{w}$	Vaghefi et al. (2010) (BEM)	4.0916	8.9751	12.5990	17.6640	39.0600
		Vaghefi et al. (2010) (FEM)	4.1215	9.0047	12.6130	17.7110	39.1550

		Akavci and Tanrikulu(2015) ($\varepsilon_z \neq 0$)	3.8333	8.8724	12.5970	17.7440	38.3330
		Younsi et al. (2018) ($\varepsilon_z \neq 0$)	3.8345	8.8756	12.6025	17.7511	38.3451
		Present study ($\varepsilon_z = 0$)	4.1011	9.1087	12.8653	18.2171	41.0098
		Present study ($\varepsilon_z \neq 0$)	3.8265	8.8560	12.5740	17.7123	38.2668
	$\overline{\sigma}_x$ (-h/2)	Vaghefi et al. (2010) (BEM)	-15.356	-9.2902	-7.4462	-5.9410	-3.4665
		Vaghefi et al. (2010) (FEM)	-15.403	-9.2995	-7.4588	-5.9591	-3.4805
		Akavci and Tanrikulu(2015) ($\varepsilon_z \neq 0$)	-16.3220	-9.6545	-7.6944	-6.1109	-3.4530
		Younsi et al. (2018) ($\varepsilon_z \neq 0$)	-16.2898	-9.6313	-7.6770	-6.0994	-3.4504
		Present study ($\varepsilon_z = 0$)	-15.6820	-9.2913	-7.3718	-5.8141	-3.2271
		Present study ($\varepsilon_z \neq 0$)	-16.6927	-9.8955	-7.8723	-6.2318	-3.4891
0.3	$\overline{w}$	Vaghefi et al. (2010) (BEM)	0.9707	2.1378	2.9853	4.1208	8.7134
		Vaghefi et al. (2010) (FEM)	0.9732	2.1407	2.9792	4.1333	8.7293
		Zhang et al. (2014)	0.9735	2.1405	2.9795	4.1332	8.7343
		Akavci and Tanrikulu(2015) ($\varepsilon_z \neq 0$)	0.8923	2.0834	2.9602	4.1669	8.9229
		Younsi et al. (2018) ($\varepsilon_z \neq 0$)	0.8925	2.0843	2.9615	4.1685	8.9253
		Present study ($\varepsilon_z = 0$)	0.9602	2.1772	3.0822	4.3543	9.6015
		Present study ($\varepsilon_z \neq 0$)	0.8908	2.0798	2.9549	4.1595	8.9080
	$\overline{\sigma}_x$	Vaghefi et al. (2010) (BEM)	-7.223	-4.3084	-3.4496	-2.7499	-1.6449
		Vaghefi et al. (2010) (FEM)	-7.2639	-4.3378	-3.4681	-2.7673	-1.6499
		Zhang et al. (2014)	-7.1493	-4.3227	-3.4710	-2.7853	-1.6759
		Akavci and Tanrikulu(2015) ($\varepsilon_z \neq 0$)	-7.6576	-4.5062	-3.5748	-2.8235	-1.5731
		Younsi et al. (2018) ($\varepsilon_z \neq 0$)	-7.6386	-4.4941	-3.5659	-2.8175	-1.5715
		Present study ($\varepsilon_z = 0$)	-7.2499	-4.2796	-3.3846	-2.6589	-1.4605
		Present study ($\varepsilon_z \neq 0$)	-7.7999	-4.5974	-3.6421	-2.8693	-1.5869

Table 8 Comparison of the dimensionless deflection w^* of isotropic square plate subjected to uniformly distributed load.

$\overline{K}_w$	$\overline{K}_s$	$a/h = 10$				$a/h = 200$			
		Thai et al. (2013)	Al Khateeb and Zenkour (2014)	Present 2D	Present Quasi-3D	Thai et al. (2013)	Al Khateeb and Zenkour (2014)	Present 2D	Present Quasi-3D
1	5	3.3455	3.18068	3.3452	3.3302	3.2200	3.21959	3.2200	3.2117
	10	2.7504	2.61977	2.7503	2.7452	2.6684	2.66809	2.6684	2.6628
	15	2.3331	2.2253	2.3330	2.3329	2.2763	2.27602	2.2763	2.2722
	20	2.0244	1.93304	2.0243	2.0270	1.9834	1.98317	1.9834	1.9803
3^4	5	2.8421	2.70699	2.8420	2.8358	2.7552	2.75485	2.7552	2.7491
	10	2.3983	2.28765	2.3982	2.3977	2.3390	2.33866	2.3389	2.3346
	15	2.0730	1.97963	2.0729	2.0754	2.0306	2.03037	2.0306	2.0274
	20	1.8244	1.74394	1.8244	1.8286	1.7932	1.79298	1.7932	1.7907
5^4	5	1.3785	1.32344	1.3784	1.3854	1.3688	1.36864	1.3688	1.3674

	10	1.2615	1.21169	1.2614	1.2684	1.2543	1.25412	1.2542	1.2531
	15	1.1627	1.11725	1.1627	1.1694	1.1572	1.15711	1.1572	1.1562
	20	1.0782	1.03638	1.0782	1.0847	1.0740	1.07389	1.0740	1.0732

Table 9 Comparisons of non-dimensional displacements and stresses of simply supported FG rectangular plate (Al/Al_2O_3) resting on elastic foundation under uniform loads $(b = 3a, a/h = 10)$.

k	K_0	J_0	Method	u^*	v^*	w^*	σ_x^*	σ_y^*	σ_{xy}^*
0	0	0	Zenkour (2009)	0.1972	0.1022	1.2583	0.7162	0.2448	0.2893
			Thai and Choi (2014a)	0.1971	0.1022	1.2583	0.7160	0.2447	0.2890
			Present 2D	0.1972	0.1021	1.2582	0.7159	0.2442	0.2869
			Present Quasi-3D	0.1953	0.1009	1.2503	0.8755	0.4074	0.2823
	100	0	Zenkour (2009)	0.192	0.100	1.2259	0.697	0.2376	0.2843
			Thai and Choi (2014a)	0.192	0.100	1.2260	0.696	0.2375	0.2840
			Mantari and Granados	0.1910	0.0995	1.2260	0.694	0.2366	0.2795
			Present 2D	0.192	0.100	1.2259	0.696	0.2370	0.2819
			Present Quasi-3D	0.190	0.099	1.2186	0.852	0.3959	0.2774
	0	100	Zenkour (2009)	0.183	0.096	1.1662	0.661	0.2245	0.2746
			Thai and Choi (2014a)	0.183	0.096	1.1662	0.661	0.2245	0.2744
			Mantari and Granados	0.1819	0.0959	1.1662	0.659	0.2236	0.2700
			Present 2D	0.183	0.096	1.1661	0.661	0.2239	0.2723
			Present Quasi-3D	0.181	0.095	1.1599	0.809	0.3749	0.2681
	100	100	Zenkour (2009)	0.1787	0.0951	1.1382	0.645	0.2184	0.2702
			Thai and Choi (2014a)	0.1787	0.0951	1.1382	0.645	0.2183	0.2700
			Mantari and Granados	0.1776	0.0942	1.1382	0.642	0.2175	0.2656
			Present 2D	0.1787	0.0950	1.1381	0.645	0.2178	0.2679
			Present Quasi-3D	0.1772	0.0939	1.1323	0.789	0.3650	0.2638
0.5	0	0	Zenkour (2009)	0.3492	0.1810	1.9344	0.233	0.0799	0.0941
			Thai and Choi (2014a)	0.3491	0.1809	1.9345	0.233	0.0799	0.0941
			Present 2D	0.3492	0.1807	1.9343	0.233	0.0797	0.0934
			Present Quasi-3D	0.3346	0.1729	1.8995	0.276	0.1286	0.0891
	100	0	Zenkour (2009)	0.3358	0.1759	1.8590	0.224	0.0763	0.0916
			Thai and Choi (2014a)	0.3358	0.1758	1.8590	0.224	0.0763	0.0916
			Mantari and Granados	0.3342	0.1746	1.8597	0.223	0.0761	0.0905
			Present 2D	0.3358	0.1756	1.8589	0.224	0.0761	0.0910
			Present Quasi-3D	0.3221	0.1681	1.8271	0.265	0.1231	0.0867
	0	100	Zenkour (2009)	0.3120	0.1665	1.7248	0.207	0.0701	0.0871
			Thai and Choi (2014a)	0.3119	0.1665	1.7248	0.207	0.0701	0.0870
			Mantari and Granados	0.3105	0.1653	1.7254	0.206	0.0699	0.0859
			Present 2D	0.3120	0.1663	1.7247	0.207	0.0699	0.0864
			Present Quasi-3D	0.2997	0.1593	1.6980	0.245	0.1136	0.0824
	100	100	Zenkour (2009)	0.3013	0.1623	1.6640	0.1999	0.0673	0.0850
			Thai and Choi (2014a)	0.3012	0.1623	1.6640	0.1999	0.0673	0.0850
			Mantari and Granados	0.2998	0.1612	1.6646	0.199	0.0671	0.0838
			Present 2D	0.3013	0.1621	1.6639	0.1998	0.0671	0.0843
			Present Quasi-3D	0.2896	0.1554	1.6394	0.2369	0.1092	0.0805
1	0	0	Zenkour (2009)	0.4855	0.2515	2.5133	0.325	0.1111	0.1307
			Thai and Choi (2014a)	0.4854	0.2515	2.5134	0.325	0.1111	0.1306
			Present 2D	0.4854	0.2512	2.5132	0.324	0.1108	0.1298
			Present Quasi-3D	0.4544	0.2347	2.4287	0.375	0.1746	0.1209

	100	0	Zenkour (2009)	0.4617	0.2424	2.3874	0.308	0.1047	0.1263
			Thai and Choi (2014a)	0.4616	0.2424	2.3875	0.308	0.1047	0.1262
			Mantari and Granados	0.4597	0.2410	2.3875	0.307	0.1044	0.1249
			Present 2D	0.4616	0.2421	2.3873	0.308	0.1045	0.1254
			Present Quasi-3D	0.4329	0.2265	2.3115	0.356	0.1652	0.1170
	0	100	Zenkour (2009)	0.4204	0.2262	2.1702	0.279	0.0940	0.1183
			Thai and Choi (2014a)	0.4203	0.2261	2.1703	0.279	0.0940	0.1182
			Mantari and Granados	0.4186	0.2248	2.1703	0.278	0.0938	0.1169
			Present 2D	0.4204	0.2258	2.1701	0.279	0.0938	0.1174
			Present Quasi-3D	0.3955	0.2118	2.1083	0.323	0.1493	0.1097
	100	100	Zenkour (2009)	0.4023	0.2191	2.0746	0.266	0.0893	0.1148
			Thai and Choi (2014a)	0.4022	0.2190	2.0746	0.266	0.0893	0.1148
			Mantari and Granados	0.4006	0.2177	2.0746	0.265	0.0890	0.1135
			Present 2D	0.4023	0.2188	2.0745	0.266	0.0890	0.1139
			Present Quasi-3D	0.3790	0.2054	2.0184	0.309	0.1422	0.1066
2	0	0	Zenkour (2009)	0.6565	0.3401	3.2267	0.439	0.1502	0.1766
			Thai and Choi (2014a)	0.6564	0.3400	3.2266	0.439	0.1502	0.1766
			Present 2D	0.6565	0.3397	3.2266	0.439	0.1499	0.1755
			Present Quasi-3D	0.6025	0.3113	3.0706	0.4975	0.2315	0.1604
	100	0	Zenkour (2009)	0.6157	0.3245	3.0219	0.4106	0.1394	0.1690
			Thai and Choi (2014a)	0.6156	0.3244	3.0218	0.4105	0.1394	0.1690
			Mantari and Granados	0.6134	0.3227	3.0178	0.409	0.1390	0.1673
			Present 2D	0.6157	0.3241	3.0218	0.4104	0.1390	0.1679
			Present Quasi-3D	0.5669	0.2977	2.8854	0.4661	0.2160	0.1538
	0	100	Zenkour (2009)	0.5476	0.2975	2.6814	0.362	0.1217	0.1557
			Thai and Choi (2014a)	0.5475	0.2974	2.6814	0.362	0.1217	0.1557
			Mantari and Granados	0.5456	0.2959	2.6783	0.362	0.1215	0.1541
			Present 2D	0.5475	0.2971	2.6813	0.362	0.1214	0.1546
			Present Quasi-3D	0.5069	0.2740	2.5748	0.414	0.1904	0.1421
	100	100	Zenkour (2009)	0.5187	0.2861	2.5364	0.342	0.1142	0.1502
			Thai and Choi (2014a)	0.5186	0.2860	2.5364	0.342	0.1142	0.1501
			Mantari and Granados	0.5168	0.2845	2.5336	0.341	0.1139	0.1486
			Present 2D	0.5187	0.2856	2.5363	0.342	0.1138	0.1490
			Present Quasi-3D	0.4813	0.2639	2.4415	0.391	0.1794	0.1372
5	0	0	Zenkour (2009)	0.7805	0.4045	3.8517	0.522	0.1785	0.2104
			Thai and Choi (2014a)	0.7802	0.4043	3.8506	0.522	0.1785	0.2103
			Present 2D	0.7804	0.4040	3.8516	0.522	0.1781	0.2089
			Present Quasi-3D	0.7198	0.3721	3.6893	0.594	0.2765	0.1919
	100	0	Zenkour (2009)	0.7232	0.3825	3.5629	0.4816	0.1633	0.1997
			Thai and Choi (2014a)	0.7230	0.3824	3.5620	0.4816	0.1633	0.1996
			Mantari and Granados	0.7198	0.3799	3.5433	0.480	0.1628	0.1971
			Present 2D	0.7231	0.3820	3.5628	0.4816	0.1629	0.1982
			Present Quasi-3D	0.6693	0.3528	3.4247	0.5496	0.2544	0.1825
	0	100	Zenkour (2009)	0.6305	0.3456	3.0979	0.4168	0.1394	0.1815
			Thai and Choi (2014a)	0.6304	0.3455	3.0972	0.4168	0.1394	0.1814
			Mantari and Granados	0.6280	0.3434	3.0834	0.416	0.1391	0.1791
			Present 2D	0.6304	0.3451	3.0978	0.4166	0.1390	0.1800
			Present Quasi-3D	0.5868	0.3199	2.9948	0.4781	0.2194	0.1663
	100	100	Zenkour (2009)	0.5923	0.3304	2.9052	0.389	0.1294	0.1741
			Thai and Choi (2014a)	0.5922	0.3303	2.9046	0.389	0.1294	0.1740
			Mantari and Granados	0.5901	0.3283	2.8925	0.389	0.1292	0.1717
			Present 2D	0.5922	0.3298	2.9050	0.389	0.1290	0.1726
			Present Quasi-3D	0.5524	0.3063	2.8153	0.448	0.2047	0.1597